



Department of Energy

Washington, DC 20585

MAR 05 1993

Mr. Joseph J. Holonich, Director
Repository Licensing & Quality Assurance
Project Directorate
Division of High-Level Waste Management
Office of Nuclear Material Safety
and Safeguards
U.S. Nuclear Regulatory Commission
Washington, D.C. 20555

References: Ltr, Loux to Bartlett, dtd 6/16/92

Dear Mr. Holonich:

Enclosed are those references from the U.S. Department of Energy's topical report, "Evaluation of the Potentially Adverse Condition of Extreme Erosion During the Quaternary Period at Yucca Mountain, Nevada," for which copyright clearances have been acquired. A follow-up transmittal will send a small package of references for which copyright clearances are still in process. These references provide the data that the Yucca Mountain Site Characterization Project Office (YMPO) used to develop the report. The data packages used by project scientists to develop the technical basis for the report are identified in the YMPO Technical Data Catalog (TDC). The December 1992 TDC, which will be transmitted under separate cover, lists the data packages submitted as of that date. The packages supporting the erosion topical report were still being entered into YMPO's technical data management system.

The March 1993 edition of the TDC will contain a complete itemization of the data packages that are available from erosion studies. If the U.S. Nuclear Regulatory Commission (NRC) wants to acquire any data packages, we ask that the NRC use the same process as the project participants. The NRC should identify the data packages that they want in the catalog and request them through the YMPO Technical Data Manager, whereupon a separate transmittal will be arranged.

The technical assessment and supporting documentation that was conducted to qualify erosion data will be transmitted under separate cover.

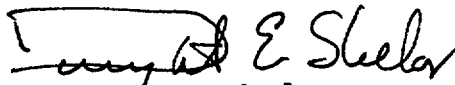
Per the request for the erosion data from the State of Nevada (reference), YMPO is transmitting this package of references separately to the State of Nevada under specific cover from YMPO. Any affected counties that would like to receive copies of these references should request them through Thomas Bjerstedt at (702) 794-7590. Data packages should be requested in writing through Ardyth M. Simmons, Technical Data Manager, at (702) 794-7998.

9303110348 930305
PDR WASTE
WM-11 PDR

102.8
WM-11
N403

If you have any questions in general, please contact Chris Einberg of my office at (202) 586-8869.

Sincerely,



Dwight E. Shelor
Associate Director for
Systems and Compliance
Office of Civilian Radioactive
Waste Management

Enclosure:
References Cited in Topical
Report

cc: w/o enclosure
C. Gertz, YMPO
T. J. Hickey, Nevada Legislative Committee
R. Loux, State of Nevada
C. Abrams, NRC
D. Bechtel, Las Vegas, NV
Eureka County, NV
Lander County, Battle Mountain, NV
P. Niedzielski-Eichner, Nye County, NV
W. Offutt, Nye County, NV
C. Schank, Churchill County, NV
F. Mariani, White Pine County, NV
V. Poe, Mineral County, NV
J. Pitts, Lincoln County, NV
J. Hayes, Esmeralda County, NV
B. Mettam, Inyo County, CA

References cited in

"EVALUATION OF THE POTENTIALLY ADVERSE CONDITION
OF EXTREME EROSION DURING THE QUATERNARY PERIOD
AT YUCCA MOUNTAIN, NEVADA"

Key to Superscripts:

- ¹ Included in this transmittal.
- ² Site Characterization Plan and documents on the controlled distribution list to NRC staff.
- ³ Copyright clearances pending.
- ⁴ Draft of in-press document.
- ⁵ NRC documents.

¹Bierman, P.R. and A.R. Gillespie, 1991. "Accuracy of Rock-Varnish Chemical Analyses: Implications for Cation-Ratio Dating", Geology, v. 19, n. 3, p. 196-199. (NNA.910923.0008)

¹Bierman, P.R., A.R. Gillespie, and S. Kuehner, 1991. "Precision of Rock-Varnish Chemical Analyses and Cation-Ratio Ages", Geology, v. 19, n. 2, p. 135-138. (NNA.921125.0004)

¹Bishop, P., 1985. "Southeast Australian Late Mesozoic and Cenozoic Denudation Rates: a Test for Late Tertiary Increases in Continental Denudation", Geology, v. 13, p. 479-482. (NNA.930216.0008)

¹Bull, W.B., 1986. "Climate-Change Induced Sediment-Yield Variations from Arid and Humid Hillslopes--Implications for Episodes of Quaternary Aggradation", Geological Society of America, Abstracts with Programs, v. 18, p. 90. (NNA.930112.0024)

³Bull, W.B., 1991. Landscape Change, Vol.1: Geomorphic Responses to Climactic Change, Oxford University Press, New York, 304 p.

¹Byers, F.M., Jr., W.J. Carr, R.L. Christiansen, P.W. Lipman, P.P. Orkild, and W.D. Quinlivan, 1976a. "Geologic Map of the Timber Mountain Caldera Area, Nye County, Nevada," Miscellaneous Investigations Series Map I-891, Scale 1:48,000, U.S. Geological Survey. (HQS.880517.1107)

¹Byers, F.M., Jr., W.J. Carr, P.P. Orkild, W.D. Quinlivan, and K.A. Sargent, 1976b. "Volcanic Suites and Related Cauldrons of the Timber Mountain-Oasis Valley Caldera Complex, Southern Nevada," U.S. Geological Survey Professional Paper 919, U.S. Government Printing Office, Washington, D.C. (NNA.870406.0239)

³Carrara, P.E., and T.R. Carroll, 1979. "The Determination of Erosion Rates from Exposed Tree Roots in the Piceance Basin, Colorado," Earth Surface Processes, v. 4, p. 307-317. (NNA.930106.0043)

³Chorley, R.J., S.A. Schumm, and D.E. Sugden, 1984. Geomorphology, Section 3.3, Denudation: The Sediment Cascade, Methuen & Co., New York, p.50-64. (NNA.930215.0054)

³Clayton, J.L. and W.F. Megahan, 1986. "Erosional and Chemical Denudation Rates in the Southwestern Idaho Batholith", Earth Surface Processes and Landforms, v. 11, p. 389-400. (NNA.930216.0053)

¹Coe, J.A., J.W. Whitney, P.A. Glancy, 1992. "Photogrammetric Analysis of Modern Hillslope Erosion at Yucca Mountain, Nevada", Geological Society of America, Abstracts

References cited in "EVALUATION OF THE POTENTIALLY ADVERSE CONDITION OF EXTREME EROSION DURING THE QUATERNARY PERIOD AT YUCCA MOUNTAIN"

with Programs, 1992 Annual Meeting, Cincinnati, OH, October 26-29, 1992, v. 24, n. 7, p. A296. (NNA.921029.0041)

¹Cole, K.L. and L. Mayer, 1982. "Use of Packrat Middens to Determine Rates of Cliff Retreat in the Eastern Grand Canyon, Arizona", Geology, v. 10, p. 597-599. (NNA.910221.0097)

¹Collins, E.W., 1982. "Surficial Evidence of Tectonic Activity and Erosion Rates, Palestine, Keechi, and Oakwood Salt Domes, East Texas", University of Texas at Austin Geological Circular 82-3, 39 p. (NNA.930216.0009)

¹Crowe, B., R. Morley, S. Wells, J. Geissman, E. McDonald, L. McFadden, F. Perry, M. Murrell, J. Poths, S. Forman, 1992. "The Lathrop Wells Volcanic Center: Status of Field and Geochronology Studies", High Level Radioactive Waste Management - Proceedings of the Third International Conference, Las Vegas, NV, April 12-16, 1992, p. 1997-2013. (NNA.920831.0001)

¹Denny, C.S. and H. Drewes, 1965. "Geology of the Ash Meadows Quadrangle, Nevada-California - Contributions to General Geology, The History of a Desert Basin and Its Bordering Highlands", U.S. Geological Survey Bulletin 1181-L, 56 p. (NNA.900104.0479)

¹Dethier, D.P., C.D. Harrington, M.J. Aldrich, 1988. "Late Cenozoic Rates of Erosion in the Western Española Basin, New Mexico - Evidence from Geologic Dating of Erosion Surfaces," Geological Society of America Bulletin, v. 100, p. 928-937, June, 1988. (NNA.921125.0007)

²DOE (U.S. Department of Energy), 1988. "Site Characterization Plan, Yucca Mountain Site, Nevada Research and Development Area, Nevada", Office of Civilian Radioactive Waste Management, Washington, D.C., DOE/RW-0199, December 1988. (HQO.881201.0002)

²DOE (U.S. Department of Energy), 1990. "Quality Assurance Requirements Document", (QARD), U.S. Department of Energy, Office of Civilian Radioactive Waste Management, DOE RW-0214, Revision 4, October 1990. (HQX.900917.0001)

²DOE (U.S. Department of Energy), 1991. "Characterization of the Meteorology for Regional Hydrology", Study Plan 8.3.1.2.1.1, U.S. Department of Energy, Office of Civilian Radioactive Waste Management, Yucca Mountain Project Office, Revision 0, March 25, 1991. (NNA.910219.0067)

¹DOE (U.S. Department of Energy), 1992. "Erosion Rates at Yucca Mountain - Technical Assessment Qualification of Data", prepared by TRW Environmental Safety Systems, Inc. for the Yucca Mountain Site Characterization Project Office, Las Vegas, NV, August 31, 1992. (NNA.921007.0095)

¹Dohrenwend, J.C., 1984. "Nivation Landforms in the Western Great Basin and Their Paleoclimatic Significance", Quaternary Research, v. 22, p. 275-288. (HQS.880517.2662)

¹Dohrenwend, J.C., S.G. Wells, B.D. Turrin, and L.D. McFadden, 1984. "Rates and Trends of Late Cenozoic Landscape Degradation in the Area of the Cima Volcanic Field, Mojave Desert California", Surficial Geology of the Eastern Mojave Desert, California - Field Trip 14, prepared for the 97th Annual Meeting of the Geological Society of America, Reno, Nevada, November 5-8, 1984, p. 101-115. (NNA.930216.0050)

¹Dohrenwend, J.C., S.G. Wells, and B.D. Turrin, 1986. "Degradation of Quaternary Cinder Cones in the Cima Volcanic Field, Mojave Desert, California", Geological Society of America Bulletin, v. 97., p. 421-427. (NNA.910123.0018)

¹Dorn, R.I., 1983. "Cation-Ratio Dating: A New Rock Varnish Age-Determination Technique", Quaternary Research, v. 20, p. 49-73. (HQS.880517.1755)

¹Dorn, R.I., and D.H. Krinsley, 1991. "Cation-Leaching Sites in Rock Varnish," Geology, v. 19, n. 11, p. 1077-1080. (NNA.930212.0013)

¹Dorn, R.I., D.B. Bamforth, T.A. Cahill, J.C. Dohrenwend, B.D. Turrin, D.J. Donahue, A.J.T. Jull, A. Long, M.E. Macko, E.B. Weil, D.S. Whitley and T.H. Zabel, 1986. "Cation-Ratio and Accelerator Radiocarbon Dating of Rock Varnish on Mojave Artifacts and Landform", Science, v. 231, p. 830-833. (NNA.910123.0019)

¹Dunne, T., M.J. Brunengo, and W.E. Dietrich, 1979. "Estimation of Cenozoic Erosion Rates from Erosion surfaces in Southern Kenya", Geological Society of America, Abstracts with Programs, 75th Annual Meeting, San Jose California, v. 11, p. 76. (NNA.930216.0004)

³Fahey, B.D. and T.H. Lefebure, 1988. "The Freeze-Thaw Weathering Regime at a Section of the Niagara Escarpment on the Bruce Peninsula, Southern Ontario, Canada", Earth Surface Processes and Landforms, v. 13, p. 293-304. (NNA.930106.0041)

¹Ford, R.L., J.P. Grimm, G.F. Martinez, J.D. Pickle, S.W. Sares, G.L. Weadock, and S.G. Wells, 1982. "A Model of Quaternary Hillslope Evolution", Geological Society of America, Abstracts with Programs, 95th Annual Meeting, October 18-21, 1982, v. 14, n. 7, p. 490. (NNA.921125.0008)

¹Frostick, L.E., and I. Reid, 1982. "Talluvial Processes, Mass Wasting and Slope Evolution in Arid Environments", Zeitschrift fur Geomorphologie N.F., supplement no. 44, p. 53-67. (NNA.930112.0022)

³Gale, S.J., 1992. "Long-Term Landscape Evolution in Australia", Earth Surface Processes and Landforms, v. 17, p. 323-343. (NNA.930216.0055)

References cited in "EVALUATION OF THE POTENTIALLY
ADVERSE CONDITION OF EXTREME EROSION DURING
THE QUATERNARY PERIOD AT YUCCA MOUNTAIN"

- ³Gerson, R., 1982. "Talus Relicts in Deserts: A Key to Major Climatic Fluctuations", Israel Journal of Earth Sciences, v. 31, p. 123-132. (NNA.930212.0016)
- ⁴Glancy, P.A., in press. "Evidence of Prehistoric Flooding and the Potential for Future Flooding at Coyote Wash, Yucca Mountain, Nevada," U.S. Geological Survey Water-Supply Paper, Denver, CO. (NNA.921027.0067)
- ³Gray, J.T., 1972. "Debris Accretion on Talus Slopes in the Central Yukon Territory", in Mountain Geomorphology: Geomorphological Processes in the Canadian Cordillera, edited by H.O. Slaymaker and H.J. McPherson, Tantalus Research Limited, Vancouver, Canada, p. 75-84 and 266-267. (NNA.930305.0102)
- ¹Gustavson, T.C. and W.W. Simpkins, 1989. "Geomorphic Processes and Rates of Retreat Affecting the Caprock Escarpment, Texas Panhandle", Bureau of Economic Geology, University of Texas at Austin, 49 p. (NNA.930112.0025)
- ¹Harrington, C.D., and J.W. Whitney, 1987. "Scanning Electron Microscope Method for Rock-Varnish Dating", Geology, v. 15, p. 967-970, October 1987. (HQS.880517.2703)
- ¹Harrington, C.D., R. Raymond, Jr., D.J. Krier, and J.W. Whitney, 1989. "Barium Concentration in Rock Varnish: Implications for Calibrated Rock Varnish Dating Curves", (abs.) Geological Society of America Abstracts with Program, v. 21, n. 6, November 9, 1989, p. A343. (NNA.910328.0051)
- ¹Harrington, C.D., D.J. Krier, R. Raymond, Jr., and S.L. Reneau, 1991. "Barium Concentration in Rock Varnish: Implications for Calibrated Rock Varnish Dating Curves", Scanning Microscopy, v. 5, n. 1, p. 55-62. (NNA.920131.0275)
- ¹Hawley, J.W., P.W. Birkeland, T.M. Oberlander, 1989. "Peer Review Report on Rock-Varnish Studies Within the Yucca Mountain Project," New Mexico Bureau of Mines and Mineral Resources, Socorro, NM, September 6, 1989. (NNA.921125.0009)
- ³Helley, E.J., 1966. "Sediment Transport in the Chowchilla River Basin - Mariposa, Madera, and Merced Counties, California," Ph.D. dissertation, University of California, Berkeley, California, p. 97-100. (NNA.930112.0020)
- ¹Hillhouse, J.W., 1987. "Late Tertiary and Quaternary Geology of the Tecopa Basin, Southeastern California", U.S. Geological Survey Miscellaneous Investigations Series Map 1-1728, 16 pp. (NNA.930106.0046)

- ¹Hoover, D.L., 1989. "Preliminary Description of Quaternary and Late Pliocene Surficial Deposits at Yucca Mountain and Vicinity, Nye County, Nevada, " U.S. Geological Survey Open-File Report 89-359, USGS-OFR-89-359, U.S. Geological Survey, Denver, CO. (NNA.900403.0406)
- ¹Huber, N.K., 1988. "Late Cenozoic Evolution of the Upper Amargosa River Drainage System, Southwestern Great Basin, Nevada and California", U.S. Geological Survey Open-File Report, USGS-OFR-87-617, 26 p., 1988. (NNA.930216.0062)
- ¹Hupp, C.R. and W.P. Carey, 1990. "Dendrogeomorphic Approach to Estimating Slope Retreat, Maxey Flats, Kentucky", Geology, v. 18, p. 658-661. (NNA.930216.0005)
- ³Kurz, M.D., 1986. "In Situ Production of Terrestrial Cosmogenic Helium and Some Applications to Geochronology", Geochimica et Cosmochimica Acta, Pergamon Journals Ltd., v. 50, p. 2855-2862. (NNA.930112.0021)
- ¹LaMarche, V.C., Jr., 1968. "Rates of Slope Degradation as Determined from Botanical Evidence, White Mountains, California," U.S. Geological Survey Professional Paper, 352-I, p. 341-377. (NNA.930212.0020)
- ¹Langbein, W.B. and S.A. Schumm, 1958. "Yield of Sediment in Relation to Mean Annual Precipitation," Transactions, American Geophysical Union, v. 39, n. 6, p. 1076-1084. (NNA.920131.0292)
- ¹Leopold, L.B., W.W. Emmett and R.M. Myrick, 1966. "Channel and Hillslope Processes in a Semiarid Area, New Mexico," Erosion and Sedimentation in a Semiarid Environment, U.S. Department of the Interior, Geological Survey Professional Paper 352-G, U.S. Government Printing Office, Washington, D.C. (NNA.920131.0294)
- ¹Marchand, D.E., 1971. "Rates and Modes of Denudation, White Mountains, Eastern California," American Journal of Science, February, 1971, v. 270, p. 109-135. (HQS.880517.1331)
- ¹McFadden, L.D., S.G. Wells, and J.C. Dohrenwend, 1986. "Influences of Quaternary Climatic Changes on Processes of Soil Development on Desert Loess Deposits of the Cima Volcanic Field, California", Catena, v. 13, p. 361-389. (HQS.880517.2759)
- ¹McGreevey, J.P. and W.B. Whalley, 1982. "The Geomorphic Significance of Rock Temperature Variations in Cold Environments, A Discussion", Arctic and Alpine Research, v. 14, p. 157-162. (NNA.930112.0023)

³Megahan, W.F., K.A. Seyedbagheri, and P.C. Dodson, 1983. "Long-Term Erosion on Granitic Roadcuts Based on Exposed Tree Roots", Earth Surface Processes and Landforms, v. 8, p. 19-28. (NNA.930216.0052)

¹Melton, M.A., 1965. "Debris-Covered Hillslopes of the Southern Arizona Desert - Consideration of Their Stability and Sediment Contribution", Journal of Geology, v. 73, p. 715-729. (NNA.930112.0019)

¹Mills, H.H., 1981. "Boulder Deposits and the Retreat of Mountain Slopes, or, "Gully Gravure" Revisited", Journal of Geology, v. 89, p. 649-660. (NNA.930106.0045)

¹Morrison, R.B., 1991. "Introduction", Quaternary Nonglacial Geology; Conterminous U.S., R.B. Morrison ed., Geological Society of America, The Geology of North America, Boulder, Colorado, v. K-2, p. 1-12. (NNA.921125.0011)

³Nesje, A., S.O. Dahl, V. Valen, and J. Øvstedal, 1992. "Quaternary Erosion in the Sognefjord Drainage Basin, Western Norway", Geomorphology, v. 5, p. 511-520. (NNA.930216.0051)

⁵NRC (U.S. Nuclear Regulatory Commission), 1983. "Staff Analysis of Public Comments on Proposed Rule 10 CFR Part 60, Disposal of High-Level Radioactive Wastes in Geologic Repositories", Office of Nuclear Regulatory Research, Washington, D.C., NUREG-0804, December, 1983.

⁵NRC (U.S. Nuclear Regulatory Commission), 1988. "Qualification of Existing Data for High-Level Nuclear Waste Repositories," Office of Nuclear Material Safety and Safeguards, W.D. Altman, J.P. Donnelly, J.E. Kennedy, Washington, D.C., NUREG-1298, February, 1988.

³Oberlander, T.M., 1972. Morphogenesis of Granitic Boulder Slopes in the Mojave Desert, California, Journal of Geology, v. 80, p. 1-20. (NNA.930112.0017)

¹Oberlander, T.M., 1974. "Landscape Inheritance and the Pediment Problem in the Mojave Desert of Southern California", American Journal of Science, v. 274, p. 849-875. (NNA.930112.0018)

¹Ohmori, H., 1983. "Characteristics of the Erosion Rate in the Japanese Mountains from the Viewpoint of Climatic Geomorphology", Zeitschrift für Geomorphologie N.F., Suppl. Bd. 46, p. 1-14. (NNA.930215.0053)

¹O'Neill, J.M., J.W. Whitney, and M.R. Hudson, 1991. "Strike-Slip Faulting and Oroclinal Bending at Yucca Mountain, Nevada - Evidence from Photogeologic and Kinematic Analysis", Geological Society of America, Abstracts with Programs, Annual Meeting, October 21-24, 1991, San Diego, California, Abstract 1384, v. 23, n. 5, p. A119. (NNA.920320.0149)

¹Palmer, A.R., 1983. Compiler, "The Decade of North American Geology, 1983 Geologic Time Scale", Geology, v. 11, n. 9, p. 503-504. (NNA.930212.0011)

³Pearce, A.J. and J.A. Elson, 1973. "Postglacial Rates of Denudation by Soil Movement, Free Face Retreat, and Fluvial Erosion, Mount St. Hilaire, Quebec", Canadian Journal of Earth Sciences, v. 10, p. 91-101. (NNA.930216.0054)

³Pierce, K.L., 1986. "Dating Methods," Active Tectonics, Chapter 13, National Academy Press, Washington, D.C., p. 195-214. (NNA.890411.0036)

¹Pierce, K.L., and S.M. Colman, 1986. "Effect of Height and Orientation (Microclimate) on Geomorphic Degradation Rates and Processes, Late-Glacial Terrace Scarps in Central Idaho", Geological Society of America Bulletin, v. 97., p. 869-885. (NNA.930216.0006)

¹Pineda, C.A., M. Peisach, and L. Jacobson, 1988. "Ion Beam Analysis for the Determination of Cation Ratios as a Means of Dating Southern African Rock Varnishes", Nuclear Instruments and Methods in Physics Research, v. B35, p. 463-466. (NNA.930106.0040)

¹Porter, S.C., 1977. "Present and Past Glaciation Threshold in the Cascade Range, Washington, U.S.A.: Topographic and Climatic Controls and Paleoclimatic Implications", Journal of Glaciology, v. 18, n. 78, p. 101-116. (NNA.930212.0022)

¹Poets, J. and F. Goff, 1990. "Using Cosmogenic Noble Gases to Estimate Erosion Rates," abstract, EOS, Transactions, American Geophysical Union, v. 71, n. 43, H52A-16, October 23, 1990. (NNA.921125.0012)

¹Prokopovich, N.P., 1987. "Rock Stripes on Sierra Nevada Foothills", California Geology, v. 40, p. 27-30. (NNA.930212.0015)

³Rapp, A. 1957. "Studien über Schutthalden in Lappland und auf Spitzbergen, mit 1 Abbildung auf Tafel und 9 Textabbildungen", Annals of Geomorphology, Bd.1, Heft 2, p. 179-200. (NNA.930226.0025)

¹Rapp, A., 1960. "Talus Slopes and Mountain Walls at Tempelfjorden, Spitsbergen - a Geomorphological Study of the Denudation of Slopes in an Arctic Locality", Det Kongelige Department for Industri og Håndverk, Norsk Polarinstitut, Skrifter, Nr. 119, 118 p. (NNA.930222.0134)

³Reneau, S.L., W.E. Dietrich, M. Rubin, D.J. Donahue, and A.J. Timothy Jull, 1989. "Analysis of Hillslope Erosion Rates Using Dated Colluvial Deposits", Journal of Geology, v. 97, p. 45-63. (NNA.930216.0048)

³Reneau, S.L. and W.E. Dietrich, 1991. "Erosion Rates in the Southern Oregon Coast Range: Evidence for an Equilibrium Between Hillslope Erosion and Sediment Yield", Earth Surface Processes and Landforms, v. 16, p. 307-322. (NNA.930216.0047)

¹Reneau, S.L. and R. Raymond, Jr., 1991. "Cation-Ratio Dating of Rock Varnish: Why Does It Work?", Geology, v. 19, n. 9, p. 937-940. (NNA.930212.0012)

³Reneau, S.L., R. Raymond, Jr., C.D. Harrington, 1992. "Elemental Relationships in Rock Varnish Stratigraphic Layers, Cima Volcanic Field, California: Implications for Varnish Development and the Interpretation of Varnish Chemistry", American Journal of Science, November, 1992, v. 292, p. 684-723. (NNA.930212.0017)

³Ritter, D.F., 1986. Process Geomorphology, Second Edition, Wm. C. Brown Publishers, Dubuque, Iowa, p. 201-204. (NNA.930215.0051)

¹Rosholt, J.N., S.M. Colman, M. Stuiver, P.E. Damon, C.W. Naeser, N.D. Naeser, B.J. Szabo, D.R. Muhs, J.C. Liddicoat, S.L. Forman, M.N. Machette, and K.L. Pierce, 1991. "Dating Methods Applicable to the Quaternary," in Morrison, R.B., ed., Quaternary Nonglacial Geology: Conterminous U.S., Geological Society of America, The Geology of North America, Boulder, Colorado, v. K-2, p. 45-74. (NNA.930305.0103)

¹Sargent, K.A., and J.H. Stewart, 1971. "Geologic Map of the Specter Range NW Quadrangle, Nye County, Nevada", U.S. Geological Survey Geologic Quadrangle Map GQ-884, scale 1:24000. (NNA.930226.0023)

³Schmidt, K.-H., 1989. "Regional Variation of Mechanical and Chemical Denudation, Upper Colorado River Basin", Earth Surface Processes and Landforms, v. 10, p. 497-508. (NNA.930216.0056)

¹Scott, R.B., 1990. "Tectonic Setting of Yucca Mountain, Southwest Nevada", Basin and Range Extensional Tectonics Near the Latitude of Las Vegas, Nevada, B.P. Wernicke, ed., Geological Society of America Memoir 176, Boulder, Colorado, p. 251-282. (NNA.910923.0009)

¹Scott, R.B., and J. Bonk, 1984. "Preliminary Geologic Map of Yucca Mountain With Geologic Sections, Nye County, Nevada", U.S. Geological Survey Open-File Report 84494, scale 1:12,000. (HQS.880517.1443)

³Sevon, W.D., 1989. "Erosion in the Juniata River Drainage Basin, Pennsylvania", Geomorphology, v. 2, p. 303-318. (NNA.930219.0014)

¹Shafer, D.S., 1986. "Paleoclimatic Significance of Late Wisconsin Cryogenic Deposits in the Central Great Basin", American Quaternary Association Program and Abstracts, Ninth Biennial Meeting, p. 163. (NNA.930212.0014)

¹Smith, G.I., V.J. Barczak, G.F. Moulton, and J.C. Liddicoat, 1983. "Core KM-3, A Surface-to-Bedrock Record of Late Cenozoic Sedimentation in Searles Lake, California", U.S. Geological Survey Professorial Paper 1256, 24 p. (NNA.900227.0061)

¹Spaulding, W.G., 1985. "Vegetation and Climates of the Last 45,000 Years in the Vicinity of the Nevada Test Site, South-Central Nevada", U.S. Geological Survey Professional Paper 1329, 83 p. (NNA.921125.0014)

¹Swadley, WC, D.L. Hoover, J.N. Rosholt, 1984. "Preliminary Report on Late Cenozoic Faulting and Stratigraphy in the Vicinity of Yucca Mountain, Nye County, Nevada", U.S. Geological Survey Open-File Report 84-788, Plate 1, 42 p., 1984. (HQS.880517.1515) (NNA.870519.0104)

¹Szabo, B.J. and J.N. Rosholt, 1991. "Conventional Uranium-Series and Uranium Trend Dating - Dating Methods Applicable to the Quaternary", Quaternary Nonglacial Geology; Conterminous U.S., edited by R.B. Morrison, Geologic Society of America, Boulder, CO, The Geology of North America, v. K-2, p. 55-60. (NNA.921125.0015)

¹Taylor, E.M., 1986. "Impact of Time and Climate on Quaternary Soils in the Yucca Mountain Area of the Nevada Test Site," Masters Thesis submitted to the Faculty of the graduate School of the University of Colorado, Department of Geological Sciences, Boulder, CO., Directed by Prof. Peter W. Birkeland, funded by the U.S. Geological Survey, Branches of Central and Western Regional Geology, May 28, 1986. (NNA.920512.0016)

¹Thordarson, W., 1983. "Geohydrologic Data and Test Results from Well J-13, Nevada Test Site, Nye County, Nevada," USGS-WRI-83-4171, Water-Resources Investigation Report, U.S. Geological Survey, Denver, CO. (NNA.870518.0071)

¹Wayne, W.J., 1982. "Fossil Patterned Ground and Rock Glaciers in the Ruby Mountains, Nevada", Geological Society of America, Abstracts with Programs, 35th Annual Meeting, Rocky Mountain Section, May 7-8, 1982, v. 14, n. 6, p. 353. (NNA.921125.0016)

⁴Whitney, J.W. and C.D. Harrington, in press. "Relict Colluvial Boulder Deposits As Paleoclimatic Indicators in the Yucca Mountain Region, Southern Nevada", preliminary draft, submitted to Geological Society of America Bulletin. (NNA.930305.0135)

¹Whitney, J.W., WC Swadley, and R.R. Shroba, 1985. "Middle Quaternary Sand Ramps in the Southern Great Basin, California and Nevada", Geological Society of America Abstracts with Programs, v. 17, n. 7, p. 750, October, 1985. (NNA.921125.0017)

¹Whitney, J.W., C.D. Harrington, and P.A. Glancy, 1988. "Deciphering Quaternary Alluvial History in Las Vegas Wash, Nevada, by Radiocarbon and Rock-Varnish Dating", Geological Society of America, Abstracts with Programs, v. 20, p. 243. (NNA.930106.0044)

¹Whitney, J.W., and D.R. Muhs, 1991. "Quaternary Movement on the Paintbrush Canyon-Stagecoach Road Fault System, Yucca Mountain, Nevada", Geological Society of America, Abstracts with Programs, v. 23, n. 5, p. A119, October, 1991. (NNA.921125.0019)

³Yair, A. and R.Gerson, 1983. "Mode and Rate of Escarpment Retreat in an Extremely Arid Environment", Annals of Geomorphology, Extreme Land Forming Events, Suppl. Bd. 21, p. 202-215. (NNA.930219.0013)

¹Young, A., 1972. Slopes, edited by K.M. Clayton, Longman, Inc., New York. (NNA.920131.0368)

Accuracy of rock-varnish chemical analyses: Implications for cation-ratio dating

Paul R. Bierman, Alan R. Gillespie

Department of Geological Sciences, University of Washington
Seattle, Washington 98195

ABSTRACT

To compare methods of rock-varnish chemical analysis and cation-ratio determination, we prepared three glass standards, synthetic analogues of rock varnish. Analysis of these standards demonstrates that material of varnishlike composition can be accurately and precisely analyzed by means of quantitative, energy-dispersive electron microscopy (SEM-EDS). However, a blind interlaboratory comparison and reexamination of published data show that most published cation ratios of varnish are probably inaccurate because the technique used most frequently to determine rock-varnish composition, proton-induced X-ray emission (PIXE), did not accurately measure the concentration of Ti in the presence of Ba, a ubiquitous component of rock varnish. This inaccuracy suggests that the premise of cation-ratio dating and dates generated by this method should be reevaluated.

INTRODUCTION

Rock-varnish cation-ratio dating of geomorphic surfaces was first proposed nine years ago (Dorn and Oberlander, 1981) and is based on the premise that in rock varnish, the ratio (Ca + K)/Ti decreases with exposure age. Numerical ages have been generated by using calibration curves constructed from cation-ratio determinations made on independently dated surfaces.

The method has been used, almost exclusively by R. I. Dorn and co-workers, to date a variety of Pleistocene and Holocene arid-region surfaces including lava flows, shorelines, alluvial fans, glacial moraines, artifacts, petroglyphs, and colluvial deposits (Dorn, 1983, 1989a, 1989b; Dorn and Oberlander, 1981; Dorn et al., 1986, 1987, 1990; Nobbs and Dorn, 1988). Results of rock-varnish cation-ratio dating have been used to revise the Sierra Nevada glacial chronology (Dorn et al., 1990), to challenge accepted petroglyph chronologies (Nobbs and Dorn, 1988) and to characterize seismic and volcanic hazards near the proposed Yucca Mountain high-level waste repository (Dorn, 1989a). Harrington and Whitney (1987), Pineda et al. (1988), Dethier et al. (1988), and Liu and Zhang (1990) have observed temporal changes in what were presumed to be three-element rock-varnish cation ratios. Of these other workers, only Dethier and Harrington have used cation ratios to date geomorphic surfaces.

Most published cation ratios (those of R. I. Dorn and co-workers) have been determined by proton-induced X-ray emission at the University of California, Davis (PIXE UCD). Cation ratios

have also been determined by electron microscopy using energy-dispersive (SEM-EDS, also referred to as SEM-EDAX) and wavelength-dispersive spectrometers (SEM-WDS) (Harrington and Whitney, 1987; Dethier et al., 1988; Dragovich, 1988; Dorn, 1989a, 1989b; Dorn et al., 1990). Dorn (1989b) and Dorn et al. (1990) determined ratios by inductively coupled argon-plasma spectroscopy (ICP). Dorn (1983) determined ratios by using X-ray fluorescence (XRF—unspecified detector).

Meaningful cation-ratio dates will be generated only if the three-element ratio (Ca + K)/Ti is accurately determined. However, the accuracy of methods used to determine this ratio has never been demonstrated by analysis of standards of varnishlike composition. Of particular concern is the accurate measurement of Ti because (1) if Ba is also present, the concentration of Ti is difficult to measure by energy-dispersive (EDS) X-ray fluorescence (XRF) techniques such as SEM-EDS, XRF-EDS, and PIXE (Fig. 1; Cahill, 1975; Harrington et al., 1990; Dorn, 1989a, 1989b; Dorn et al., 1990) and (2) published analyses of rock varnish, made by methods known to measure Ba and Ti accurately, indicate that they are both present in varnish at concentrations of 5000 to 15000 ppm (Engle and Sharp, 1958; Bard, 1979; Dragovich, 1988; Harrington et al., 1990; Dorn, 1980, 1989b; Dorn et al., 1990; Raymond et al., 1990). Ba does not affect Ti measurements made by neutron-activation analysis (NAA), ICP, SEM-WDS, and XRF-WDS.

Because we are using SEM-EDS (Bierman et

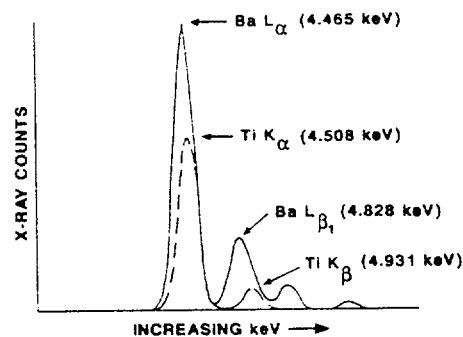


Figure 1. Ti K and Ba L peaks overlap in energy-dispersive X-ray spectra. If Ba peaks are not deconvolved, apparent Ti K_{α} (4.508 keV) and K_{β} (4.931 keV) peaks shift to lower energies as they are superimposed upon Ba L_{α} (4.465 keV) and L_{β} (4.828 keV) peaks.

al., 1991) to determine varnish chemistry and because the accuracy of SEM-EDS measurements of Ti has been questioned (Dorn, 1989a, 1989b; Dorn et al., 1990), we prepared standards of specific composition to test the accuracy of our analyses. To allow meaningful comparison of our SEM measurements of varnish chemistry with those made by other methods, we conducted a blind interlaboratory test. We used synthetic varnish standards because, in contrast to natural varnish, these standards are of known composition.

METHODS

Using reagent-grade chemicals, we prepared three glass analogues of rock varnish spanning

Note: Additional material for this article is Supplementary Data 9108, available on request from the GSA Documents Secretary (see footnote 1).

the range of Ba/Ti and cation ratios measured in natural varnish. In a blind test, aliquots of the glasses were analyzed by XRF-WDS, ICP, PIXE UCD, and PIXE microprobe (PIXE MCP). We analyzed other aliquots at the University of Washington (UW) by quantitative SEM-EDS and SEM-WDS.¹ Varnish standards are available from Bierman.

ANALYTICAL RESULTS AND DISCUSSION

The chemical composition and cation ratios of synthetic rock-varnish standards determined

by quantitative, standard-based SEM-EDS agree with known compositions and are similar to those determined by most other methods (Table 1, Fig. 2).

However, our interlaboratory comparison shows that cation ratios and concentrations measured by PIXE UCD are inaccurate (Table

1, Fig. 2). There are two sources of error in PIXE UCD cation-ratio determinations, (Ca + K) and Ti. The error in (Ca + K) is similar for all three synthetic varnishes, is not correlated with Ba content, and averages 16%; in contrast, the

Figure 2. SEM-EDS cation ratios are accurate and comparable to those measured by all other methods except PIXE UCD. PIXE UCD error increases with Ba/Ti ratio, suggesting that Ba, included in Ti abundances, lowers cation ratio. Uncertainties, calculated according to Bierman et al. (1991), are shown if they exceed width of symbol. Ratios in same order for FV-1 and FV-3 as for FV-2. CR = cation ratio, (K + Ca)/Ti.

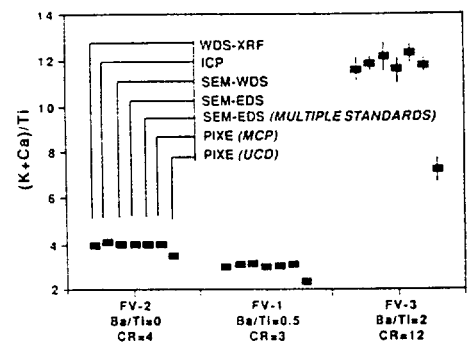


TABLE 1. COMPOSITION OF SYNTHETIC VARNISH STANDARDS

TECHNIQUE: LAB:	MIXTURE	XRF/WDS LANL	ICP UW	SEM/WDS UW	SEM/EDS ⁺ UW	SEM/EDS ⁺ UW	PIXE/MCP LANL	PIXE UCD
Glass FV-1 (Ba/Ti = 0.5)								
Number of analyses:		1	6	12	8	11	3	5
SiO ₂	49.54	48.36 +/- 0.44	48.64 +/- 0.13	48.39 +/- 0.21	48.12 +/- 0.33	49.24 +/- 0.24	NA	25.05 +/- 1.61
Al ₂ O ₃	22.92	23.11 +/- 0.13	22.54 +/- 0.03	22.90 +/- 0.11	22.67 +/- 0.19	23.52 +/- 0.12	NA	14.12 +/- 1.06
Fe ₂ O ₃	11.83	11.96 +/- 0.28	11.71 +/- 0.05	11.46 +/- 0.11	12.07 +/- 0.15	11.65 +/- 0.1	NA	10.68 +/- 2.09
MnO	7.12	7.76 +/- 0.01	7.62 +/- 0.05	7.61 +/- 0.05	8.39 +/- 0.05	7.51 +/- 0.04	NA	7.62 +/- 1.19
MgO	1.83	1.89 +/- 0.69	1.87 +/- <.01	1.89 +/- 0.01	1.70 +/- 0.03	1.84 +/- 0.05	NA	<0.06
TiO ₂	1.84	1.85 +/- 0.03	1.75 +/- 0.01	1.74 +/- 0.04	1.95 +/- 0.03	1.91 +/- 0.02	2.13 +/- 0.02	1.91 +/- 0.11
BaO	0.62	0.54 +/- 0.01	0.54 +/- <.01	0.58 +/- 0.02	0.54 +/- 0.03	0.63 +/- 0.02	0.59 +/- 0.02	<0.02
K ₂ O	1.99	1.95 +/- 0.02	1.89 +/- 0.04	1.96 +/- 0.01	2.10 +/- 0.03	1.98 +/- 0.02	2.46 +/- 0.05	1.60 +/- 0.08
CaO	2.31	2.38 +/- 0.06	2.40 +/- <.01	2.35 +/- 0.01	2.45 +/- 0.01	2.32 +/- 0.02	2.72 +/- 0.05	1.87 +/- 0.09
Na ₂ O	0.00	0.10 +/- 0.20	0.18 +/- <.01	NA	NA	0.21 +/- 0.03	NA	<0.25
TOTAL	100.00	99.90	99.14	98.88	100.00	100.60		62.85
(K+Ca)/Ti &	3.00	3.00 +/- 0.07	3.13 +/- 0.03	3.17 +/- 0.07	3.00 +/- 0.05	3.05 +/- 0.04	3.12 +/- 0.05	2.33 +/- 0.16
(K+Ca)/Ti #		(n = 1)	**	3.18 +/- 0.09	3.00 +/- 0.03	3.05 +/- 0.04	3.11 +/- 0.07	2.32 +/- 0.05
Glass FV-2 (Ba/Ti = 0)								
Number of analyses:		1	6	12	8	10	3	5
SiO ₂	50.96	49.64 +/- 0.44	49.58 +/- 0.02	49.27 +/- 0.75	48.98 +/- 1.32	50.27 +/- 0.88	NA	27.82 +/- 2.78
Al ₂ O ₃	22.78	23.20 +/- 0.13	22.60 +/- 0.03	23.14 +/- 0.22	22.98 +/- 0.78	23.93 +/- 0.54	NA	15.29 +/- 1.78
Fe ₂ O ₃	11.74	12.03 +/- 0.28	11.65 +/- 0.06	11.49 +/- 0.15	12.00 +/- 0.28	11.73 +/- 0.21	NA	13.31 +/- 2.95
MnO	7.07	7.74 +/- 0.01	7.57 +/- 0.07	7.67 +/- 0.03	8.38 +/- 0.11	7.58 +/- 0.12	NA	7.45 +/- 1.65
MgO	1.82	1.98 +/- 0.69	1.85 +/- <.01	1.90 +/- 0.02	1.75 +/- 0.14	1.98 +/- 0.06	NA	<0.06
TiO ₂	1.37	1.38 +/- 0.03	1.32 +/- 0.01	1.36 +/- 0.04	1.44 +/- 0.03	1.36 +/- 0.02	1.56 +/- 0.02	1.31 +/- 0.14
BaO	0.00	<0.01	<0.02	<0.02	<0.02	<0.03	<0.006	<0.02
K ₂ O	1.98	1.90 +/- 0.02	1.86 +/- 0.05	1.93 +/- 0.03	2.04 +/- 0.09	1.92 +/- 0.07	2.22 +/- 0.03	1.62 +/- 0.13
CaO	2.30	2.37 +/- 0.06	2.41 +/- 0.02	2.35 +/- 0.02	2.44 +/- 0.03	2.32 +/- 0.03	2.65 +/- 0.09	1.97 +/- 0.19
Na ₂ O	0.00	0.04 +/- 0.20	0.27 +/- 0.20	NA	NA	0.19 +/- 0.03	NA	<0.25
TOTAL	100.00	100.28	99.11	99.11	100.01	101.07		68.77
(K+Ca)/Ti &	4.00	3.98 +/- 0.10	4.13 +/- 0.06	4.03 +/- 0.12	3.99 +/- 0.12	4.01 +/- 0.09	4.00 +/- 0.09	3.51 +/- 0.44
(K+Ca)/Ti #		(n = 1)	**	4.02 +/- 0.09	3.98 +/- 0.08	4.01 +/- 0.09	3.99 +/- 0.07	3.51 +/- 0.14
Glass FV-3 (Ba/Ti = 2)								
Number of analyses:		1	6	12	10	8	3	5
SiO ₂	51.11	49.83 +/- 0.44	50.09 +/- 0.26	49.21 +/- 0.61	49.81 +/- 0.37	50.95 +/- 0.24	NA	28.73 +/- 1.98
Al ₂ O ₃	22.83	23.20 +/- 0.13	22.57 +/- 0.33	22.78 +/- 0.11	22.60 +/- 0.15	23.56 +/- 0.08	NA	15.84 +/- 1.15
Fe ₂ O ₃	11.78	11.95 +/- 0.28	11.73 +/- 0.04	11.47 +/- 0.11	12.05 +/- 0.18	11.73 +/- 0.1	NA	14.98 +/- 1.47
MnO	7.09	7.74 +/- 0.01	7.58 +/- 0.05	7.57 +/- 0.04	8.35 +/- 0.05	7.52 +/- 0.03	NA	8.36 +/- 0.78
MgO	1.82	1.79 +/- 0.69	1.78 +/- <.01	1.82 +/- 0.01	1.62 +/- 0.05	1.87 +/- 0.08	NA	<0.06
TiO ₂	0.46	0.47 +/- 0.03	0.46 +/- 0.01	0.45 +/- 0.04	0.50 +/- 0.03	0.44 +/- 0.02	0.57 +/- 0.01	0.63 +/- 0.05
BaO	0.61	0.55 +/- 0.01	0.54 +/- <.01	0.57 +/- 0.02	0.57 +/- 0.02	0.64 +/- 0.05	0.68 +/- 0.01	<0.02
K ₂ O	1.98	1.92 +/- 0.02	1.88 +/- 0.04	1.94 +/- 0.02	2.09 +/- 0.03	1.96 +/- 0.01	2.49 +/- 0.04	1.64 +/- 0.14
CaO	2.31	2.35 +/- 0.06	2.39 +/- 0.01	2.34 +/- 0.01	2.42 +/- 0.01	2.28 +/- 0.01	2.74 +/- 0.06	1.90 +/- 0.17
Na ₂ O	0.00	0.08 +/- 0.20	0.26 +/- 0.20	NA	NA	0.22 +/- 0.04	NA	<0.25
TOTAL	100.00	99.88	99.28	98.15	100.01	100.95		72.08
(K+Ca)/Ti &	12.00	11.63 +/- 0.76	11.86 +/- 0.28	12.18 +/- 1.08	11.57 +/- 0.70	12.30 +/- 0.53	11.79 +/- 0.26	7.21 +/- 0.73
(K+Ca)/Ti #		(n = 1)	**	12.40 +/- 1.11	11.64 +/- 0.35	12.34 +/- 0.55	11.76 +/- 0.06	7.22 +/- 0.17

Note: Uncertainties are one sample standard deviation except for XRF/WDS for which long-term average uncertainties are stated. NA = not analyzed.

& Cation ratio determined from average values for Ti, Ca, and K; uncertainty from standard error propagation (Bierman et al., 1991).

Cation ratio is average of multiple determinations; uncertainty is one sample standard deviation.

** Data reduction does not provide results for individual analyses.

* Multiple standards used for calibration.

+ Results normalized to 100%.

error in PIXE UCD Ti measurements is proportional to the amount of Ba in the synthetic varnish. For synthetic varnish FV-2, which contains no Ba, the measured concentration of Ti is 5% lower than the known value; it is 4% higher if Ba/Ti = 0.5 (FV-1) and 37% higher if Ba/Ti = 2 (FV-3). The undetected Ba in FV-1 and FV-3 lowers the cation ratio by raising the apparent concentration of Ti. For FV-2 (no Ba), cation ratios determined by PIXE UCD are 12% lower than the known value. PIXE UCD cation ratios are 23% lower for Ba/Ti = 0.5 (FV-1) and 40% lower for Ba/Ti = 2 (FV-3).

A shift in apparent Ti peak position, proportional to the amount of Ba in the synthetic varnish, indicates that PIXE UCD cation ratios are inaccurate primarily because Ba L_{α} and L_{β} X-ray counts are assigned to the Ti K_{α} and K_{β} X-ray peaks (Fig. 3). T. Cahill (1990, personal commun.) has suggested that by assuming the observed shift is a linear function of concentration and by incorporating a factor for the efficiency of X-ray generation, Ba/Ti can be estimated. Using this method, we calculated Ba/Ti ratios of 0.63 for FV-1 (Ba/Ti = 0.50) and 3.15 for FV-3 (Ba/Ti = 2.00). There is no indication that peak shift has ever been used to deconvolve PIXE spectra of rock varnish.

Although we attempted to duplicate the protocol used to generate previous PIXE UCD varnish analyses by contacting Dorn and by working with UCD, there may be minor and apparently inconsequential differences between our protocol and that used for previous varnish analyses: (1) Samples of synthetic varnish were mounted by UCD personnel, using a different substrate (Mylar) and adhesive (Apeizon) than that used by Dorn (Kapton and unspecified adhesive). (2) Synthetic varnish grains (5–20 μm) may be larger than those used by Dorn, although the magnitude of this discrepancy cannot be determined because the particle size used for previous PIXE varnish analyses has not been stated explicitly. (3) Our analyses were matrix corrected with the RACE program (Cahill,

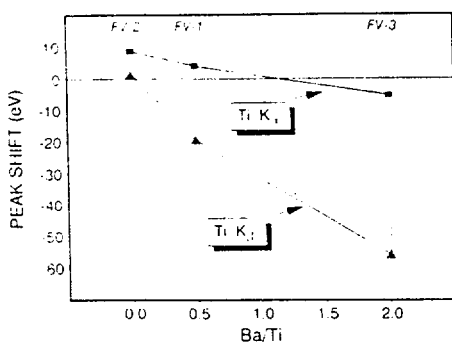


Figure 3. Center of apparent Ti K_{α} and L_{β} peaks undetected by PIXE UCD (see Fig. 1). Mean and sample standard deviation, five replicate analyses for each synthetic varnish.

1975) assuming a particle size of 8–16 μm , and it has not been specified whether matrix corrections were used for previous PIXE varnish analyses. (4) Although standards were run with our PIXE analyses, we present uncorrected PIXE data because there is no indication that previous PIXE rock-varnish analyses were corrected to standards.

T. Cahill, director of the Crocker Nuclear Lab (UCD), suggested (1990, personal commun.) how these differences might affect our analyses: (1) Substrate and adhesive are unimportant because PIXE spectra are blank corrected. (2) Grain size and matrix correction will preferentially affect concentrations reported for light elements such as Na, Mg, Si, and Al; values reported for heavier elements, such as Ti, Fe, Mn, and Ba, are less sensitive to grain size and matrix correction; the effects on (Ca + K) are moderate but must be $\leq 16\%$, the difference between PIXE UCD and the mixture values for the glasses. (3) Because Ba was not detected by PIXE UCD analyses, its concentration cannot be modified by matrix or standard correction.

Any errors in PIXE UCD analyses of synthetic varnish related to the above-mentioned factors are subordinate to those caused by inadequate Ba-Ti deconvolution because (1) the inaccuracy of Ti and cation-ratio measurements is proportional to the Ba/Ti ratio (Fig. 2) and (2) the Ba-dependent inaccuracy of Ti equals or exceeds the Ba-independent inaccuracy of (Ca + K) at Ba concentrations typical of rock varnish. It is important to consider that RACE software used at UCD was designed and tested not for analysis of compositionally complex geologic materials but for the analysis of $< 1\text{-}\mu\text{m}$ atmospheric particles of simple composition (T. Cahill, 1990, personal commun.).

IMPLICATIONS

Analysis of rock-varnish standards shows that quantitative SEM-EDS can accurately determine the abundance of Ba and Ti at concentrations typical of rock varnish if reference spectra are used for deconvolution. This finding supports Harrington et al. (1990) and contradicts Dorn (1989a, 1989b) and Dorn et al. (1990). Dorn has not specified the software, equipment, or operating conditions he used to make SEM-EDAX (EDS) measurements; however, his SEM-EDAX protocol must differ from that used in this study and in Harrington et al. (1990) because of its stated inability to deconvolve Ba-Ti X-rays.

Our analyses of synthetic rock varnish support assertions of Harrington et al. (1990) and suggest that most published cation ratios are inaccurate, because PIXE UCD was incapable of measuring accurately the concentration of Ti in the presence of Ba. This inaccuracy is specific to the UCD RACE program, rather than the PIXE method, because PIXE microprobe software

used by Los Alamos National Laboratory (LANL, Table 1) can accurately deconvolve Ba and Ti X-rays.

Published data support our finding that PIXE UCD analyses are flawed. Dorn et al. (1990, Fig. 4b) reported that of > 100 rock-varnish samples collected from the Coso Range and analyzed by ICP, most contain Ba (median concentration Ba ≈ 0.5 wt%). However, Dorn (1989a) also demonstrated that cation ratios of varnish samples collected from 16 calibration sites in the Coso Range and analyzed by both PIXE and SEM-EDAX were well correlated (Fig. 4). Because Dorn has not been able to separate Ba and Ti with SEM-EDAX deconvolution programs (Dorn et al., 1990, p. 4), the correlation between PIXE and SEM-EDAX suggests that both methods included Ba X-rays in the Ti peak, raising the apparent concentration of Ti and lowering the calculated cation ratio.

The problem of correctly deconvolving Ba and Ti X-rays is not limited to PIXE UCD or to the SEM-EDAX software used by Dorn; most, if not all, previously published cation-ratio calibration curves appear to be similarly flawed. Ba and Ti were not deconvolved in either Harrington and Whitney (1987) or Dethier et al. (1988) (see Harrington et al., 1990). Data of Pineda et al. (1988) show the apparent Ti peak shift we observed, and Liu and Zhang (1990) did not mention deconvolution of Ba and Ti.

Only a few published analyses of rock varnish are unaffected by problems in measurement of Ti and Ba. Bard (1979) scraped varnish from petroglyphs of well-documented typological age and measured the abundance of 32 elements using NAA (not susceptible to Ba-Ti overlap); only Ba showed a simple trend with typological age (Fig. 5). Although Dorn (1983, p. 50) suggested that the ratio of Ca/Ti should decrease with age, Bard's data show no such trend.

Concentrations of Ba and Ti are not strongly

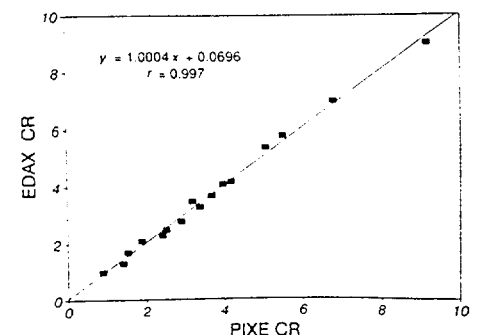
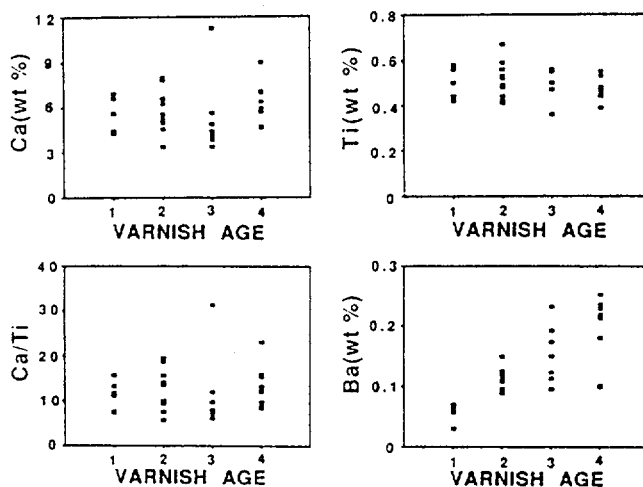


Figure 4. PIXE UCD and SEM-EDAX cation ratios (CR) from 16 sites in Coso Range (Dorn, 1989a, Table 3). Because Coso varnishes contain Ba (Dorn et al., 1990) and because SEM-EDAX used by Dorn (1989a, 1989b) cannot deconvolve Ba and Ti X-rays, this correlation suggests that PIXE UCD is also incapable of accurately measuring Ti in presence of Ba.

Figure 5. NAA data from Bard (1979, Table 19). Relative varnish age (1 = youngest, 4 = oldest) based on typological analysis of petroglyphs from which it was scraped. No change with assumed age is shown for Ca, Ti, or Ca/Ti, a ratio that should decrease with age (Dorn, 1983). Ba increases with age.



correlated in rock varnish (S. Reneau, 1990, personal commun.), so it is not possible to correct published cation ratios retrospectively for previously undetected Ba. Nor is it possible to replicate previously published, Ba-contaminated, three-element curves by using an accurately determined four-element ratio $(Ca + K)/(Ti + Ba)$ (S. Reneau, 1990, personal commun.). However, Raymond et al. (1990) have shown a strong spatial correlation between the concentration of Ba and Mn in rock varnish; this suggests that changes in Mn concentration could affect cation ratios. We and workers at Los Alamos are testing the temporal significance of Raymond et al.'s observations.

The effect of inaccurate chemical analyses on the accuracy of published cation-ratio dates is not clear. Previous workers have found a systematic change with time in what were previously assumed to be three-element cation ratios, despite or because of the inclusion of an undetermined amount of Ba. However, the apparent inaccuracy of previous analyses, the lack of standards of varnishlike composition, and the ubiquitous presence of Ba in rock varnish cast doubt on the empirically determined central premise of cation-ratio dating, the systematic change in a three-element cation ratio. It is possible that Ba, either alone or coupled with changes in Mn, Ca, K, and Ti, could account for the apparent temporal trends in cation ratios. Because of these uncertainties and because there is no theoretical or experimental verification that the ratio of $(Ca + K)/Ti$ changes with time in varnish, we suggest that the basic assumptions underlying the use of the cation-ratio method as a dating tool be reexamined. We urge caution in the acceptance and use of existing cation-ratio ages.

NOTE ADDED AFTER REVIEW

Concurrent with submission of this paper for review, we made available to participating laboratories the results of all analyses. Subsequently, T. Cahill (director, Crocker Nuclear

Lab, UCD) notified us that a change had been made to the RACE program (September 1990) that allowed Ba to be identified in at least two of our 15 samples. He suggested that the ability to discriminate Ba was diminished when the UCD PIXE system was reconfigured in late 1986. The efficiency of Ba-Ti deconvolution by RACE prior to 1986 cannot be determined rigorously because the system and the computer code used to analyze spectra have been dismantled; however, the close correlation between Dorn's SEM-EDAX and PIXE data for the Coso Range (Fig. 4) strongly suggests that Ba and Ti were not accurately deconvolved by PIXE UCD even before the 1986 reconfiguration.

REFERENCES CITED

- Bard, J.C., 1979, The development of a patination dating technique for Great Basin petroglyphs using neutron activation and X-ray fluorescence analysis [Ph.D. thesis]: Berkeley, University of California, 409 p.
- Bierman, P.R., Gillespie, A.R., and Kuehner, S.M., 1991, Precision of rock-varnish cation-ratio ages: *Geology* (in press).
- Cahill, T.A., 1975, Ion excited X-ray analysis of environmental samples, in Ziegler, J.F., ed., *New uses of ion accelerators*: New York, Plenum, p. 1-67.
- Dethier, D.P., Harrington, C.D., and Aldrich, M.J., 1988, Late Cenozoic rates of erosion in the western Espanola Basin, New Mexico: Evidence from geologic dating of erosion surfaces: *Geological Society of America Bulletin*, v. 100, p. 928-937.
- Dorn, R.I., 1980, Characteristics and origin of rock varnish [B.S. thesis]: Berkeley, University of California, 409 p.
- 1983, Cation-ratio dating: A new rock varnish age-determination technique: *Quaternary Research*, v. 20, p. 49-73.
- 1989a, A critical evaluation of cation-ratio dating of rock varnish, and evaluation of its application to the Yucca Mountain repository by the Department of Energy and its subcontractors, in Nevada nuclear waste site investigation, Evaluation of the geologic relationships and seismotectonic stability of the Yucca Mountain area: Reno, Nevada, Mackay School of Mines, Appendix A.
- 1989b, Cation-ratio dating of rock varnish: A geographic assessment: *Physical Geography*, v. 13, p. 559-596.

- Dorn, R.I., and Oberlander, T.M., 1981, Rock varnish origin, characteristics and usage: *Zeitschrift für Geomorphologie*, v. 25, p. 420-436.
- Dorn, R.I., and 11 others, 1986, Cation-ratio and accelerator radiocarbon dating of rock varnish on Mojave artifacts and landform surfaces: *Science*, v. 231, p. 830-833.
- Dorn, R.I., Turrin, B.D., Jull, A.J., Linick, T.W., and Donahue, D.J., 1987, Radiocarbon and cation-ratio ages for rock varnish on Tioga and Tahoe morainal boulders of Pine Creek, eastern Sierra Nevada, California, and their paleoclimatic implications: *Quaternary Research*, v. 28, p. 38-49.
- Dorn, R.I., Cahill, T.A., Eldred, R.A., Gill, T.E., Kushko, B.H., Bach, A.J., and Elliot-Fisk, D.L., 1990, Dating rock varnish by the cation ratio method with PIXE ICP, and the electron microprobe: *International Journal of PIXE*, v. 1.
- Dragovich, D., 1988, A preliminary electron probe study of microchemical variations in desert varnish in western New South Wales, Australia: *Earth Surface Processes and Landforms*, v. 13, p. 259-270.
- Engle, C.G., and Sharp, R.P., 1958, Chemical data on desert varnish: *Geological Society of America Bulletin*, v. 69, p. 487-518.
- Harrington, C.D., and Whitney, J.W., 1987, Scanning-electron microscope method for rock varnish dating: *Geology*, v. 15, p. 967-970.
- Harrington, C.D., Reneau, S.L., Raymond, R., and Krier, D.J., 1990, Barium concentrations in rock varnish: Implications for calibrated rock-varnish dating curves: *Scanning Microscopy International*.
- Liu, T., and Zhang, Y., 1990, Establishment of a cation-leaching curve of varnish for the Dunhuang region, western China (in Chinese, translation supplied by R. I. Dorn, 1989): *Seismology and Geology*.
- Nobbs, M., and Dorn, R.I., 1988, Age-determinations for rock varnish formation with petroglyphs: Cation-ratio dating of 24 motifs from the Olary region of arid south Australia: *Rock Art Research*, v. 5, p. 108-146.
- Pineda, C.A., Peisach, M., and Jacobson, L., 1988, Ion beam analysis for the determination of cation-ratios as a means of dating southern African rock art: *Nuclear Instruments and Methods in Physics Research*, v. B35, p. 463-466.
- Raymond, R., Reneau, S.L., and Harrington, C.D., 1990, Elemental relationships as seen with SEM/EDX elemental line profiling: *Scanning Microscopy International*.

ACKNOWLEDGMENTS

Supported by U.S. Geological Survey Grant 14-08-0001-G1783 and National Science Foundation Grant EAR-9004252 to Gillespie and Bierman. We thank T. Gill, T. Cahill, and B. Perley (PIXE UCD), G. Ludeman (XRF Los Alamos), S. Kuehner (SEM UW), P. Rogers (PIXE microprobe Los Alamos), and A. Irving (ICP UW). Our understanding of analytical systems was furthered by discussions with R. Hagan and T. Benjamin. We thank I. McCallum and A. Irving for assistance in synthetic varnish preparation; C. Harrington for suggesting synthetic varnish; R. Dorn for alerting us to the "barium problem"; and T. Dunne, B. Atwater, S. Kuehner, S. Reneau, C. Harrington, S. Porter, R. Hagan, D. Clark, J. Adams, E. Shock, G. Morgan, and T. Swanson for helpful reviews.

Manuscript received August 27, 1990

Revised manuscript received November 5, 1990

Manuscript accepted November 21, 1990

Precision of rock-varnish chemical analyses and cation-ratio ages

Paul R. Bierman, Alan R. Gillespie, Scott Kuehner

Department of Geological Sciences, University of Washington, Seattle, Washington 98195

ABSTRACT

New data and statistical analyses indicate that the precision of the mean rock-varnish cation ratio determined for a geomorphic surface and the uncertainty of the age calculated from that ratio are controlled by the area of varnish included in each chemical analysis, the precision with which each cation ratio is determined, and the number of independent chemical analyses. This study has implications for the interpretation of published cation-ratio ages and the future use of cation-ratio dating.

INTRODUCTION

Rock varnish is a <200 μm layer composed primarily of Al, Si, Fe, and Mn oxides. Varnish chemistry may change predictably with time (Bard, 1979). Dorn (1983, 1989) and Harrington and Whitney (1987) have reported that the ratio $(\text{K} + \text{Ca})/\text{Ti}$ in varnish (the cation ratio) decreases logarithmically with estimated exposure age; they argued that this decrease reflects preferential leaching of K and Ca relative to Ti. Empirical calibration curves have been constructed so that exposure ages may be estimated.

Cation ratios have been determined by three methods. Dorn (1983, 1989) scraped <1 to >50 cm^2 of varnish from numerous rocks and used proton-induced X-ray emission at the University of California, Davis (PIXE UCD), to analyze three to five homogenized samples from each deposit. Harrington and Whitney (1987) used a scanning electron microscope and energy-dispersive spectrometer (SEM-EDS) to analyze varnish in situ at 70 to 90 places (each 10–100 mm^2) on the surface of 8 to 10 samples from each deposit. Dragovich (1988) and Dorn (1989) used a SEM and wavelength-dispersive spectrometer (SEM-WDS = electron microprobe) to determine ratios at points (<2000 μm^2) in varnish cross sections.

The cation-ratio dating method is only calibrated empirically; the processes responsible for the reported change in ratios over time are not understood, and the method lacks an accepted protocol for calculating representative age uncertainties. Prior research has established neither the size nor the number of varnish samples that must be analyzed in order to characterize precisely and accurately the cation ratio that best represents the exposure age of a geomorphic surface.

We present a statistical analysis of cation-ratio precision that is applicable regardless of the method used to measure varnish composition. We do not consider possible problems with the methods employed to determine cation ratios nor with the premise of cation-ratio dating. In

addition, if cation ratios are used to generate numerical rather than relative ages, the precision and accuracy of calibration must also be considered when calculating the uncertainty of a cation-ratio age (cf. Harden et al., 1988).

METHODS

Using a rock drill, we collected varnish from boulders on the rim of Fish Springs cinder cone near Big Pine, California (314 ± 18 ka; Martel et al., 1987), and from the Bishop Tuff 8 km east-northeast of the town of Rovanna (708 ± 15 ka; Bailey et al., 1976). Chemical analyses were made of the varnish surface with a Tracor Northern EDS mounted on a JEOL 733 using a 15 keV accelerating voltage and a 10 nA beam current (measured on a Faraday cup). Reference spectra were used in the EDS deconvolution routine (Tracor Northern FIT program). We made quantitative analyses of Si, Al, Fe, Mn, Mg, Ba, Ti, Ca, and K by using the Tracor Northern ZAF procedure for matrix correction.

After examining the varnish surface with

backscattered-electron detectors, which allow identification and avoidance of substrate or microcolonial fungi, we selected 19.6 mm^2 areas for analysis. We analyzed varnish at the 19 locations four times, changing the area over which the electron beam was scanned from 6.0 to 0.99 to 0.062 to 0.002 mm^2 . Duplicate analyses showed no significant machine drift.

Nomenclature is summarized in Appendix 1. Introductory texts, such as Freund (1988), provide detailed explanations of the statistical concepts we use.

MEASUREMENTS AND STATISTICAL ANALYSES RELEVANT TO CATION-RATIO PRECISION

Most geomorphic surfaces are heterogeneous with reference to factors that have been hypothesized by Dorn (1989) to affect cation ratios (e.g., dust flux, precipitation, orientation, vegetation). According to Dorn and Oberlander (1982, p. 321) varnish growth is time transgressive with "many thousands of years required to develop a complete coat." In addition, rock surfaces erode and are revarnished, creating a patchwork of varnish populations at various scales—each of a different age and each, if cation leaching is occurring, having a different true or population mean cation ratio, μ_{CR} .

Because the above-mentioned processes cause varnish on every geomorphic surface to be chemically heterogeneous, understanding the na-

TABLE 1. COMPARISON OF ROCK VARNISH CHEMICAL ANALYSIS TECHNIQUES

Analytical instrument, dwell time (s)	X-ray detector	Approximate analytical uncertainty for rock varnish (%)			Calculated $(\text{Ca}+\text{K})/\text{Ti}$ uncertainty* (%)	Measured or reported cation ratio uncertainty
		Ti	Ca	K		
PIXE, 100	EDS	8 [†]	6 [†]	6 [†]	9	9-12 [‡]
PIXE, 100	EDS	6-11 [#]	5-10 [#]	5-8 [#]	7-12	2-4 [#]
SEM, 200	EDS	10	2.5	1.5	10.3	10.5 ^{**}
SEM, 4000	EDS	1-2	0.5	0.5	≤ 2	No data
SEM, 40	WDS	8-12	2-3	2-3	10-12	No data
SEM, 800	WDS	1-2	0.5	0.5	≤ 2	No data

Note: PIXE is proton induced X-ray emission; SEM is scanning electron microscope; EDS is energy dispersive spectrometer; WDS is wavelength dispersive spectrometer.

* Calculated by using equation 1 (see text).

[†] T. Gill (1989, personal commun.).

[‡] Data from Nobbs and Dorn (1988, Table 2).

[#] Range of uncertainty (1 σ , 5 blind replicates of each of 3 synthetic rock varnishes).

** See Figure 1, this paper.

ture and scale of this variability is prerequisite to collecting meaningful cation-ratio data. The data and statistical analysis that follow begin a rigorous identification of the appropriate scale for cation-ratio sampling and, if the cation-ratio dating is valid, suggest a method to calculate the number and precision of ratio determinations necessary to solve specific geologic problems.

Precision of Each Cation-Ratio Determination

Standard error-propagation theory may be used to calculate the precision of each cation-ratio (CR) determination based on the analytic precision of individual cation analyses:

$$\sigma_{CR} = CR \left[\frac{(\sigma_{Ca}^2 + \sigma_{K}^2)}{(Ca + K)^2} + \frac{\sigma_{Ti}^2}{Ti^2} \right]^{0.5} \quad (1)$$

Table 1 lists the average precision with which K, Ca, and Ti (at concentrations typically measured in rock varnish) are determined by a single PIXE or SEM analysis. Because the probability of X-ray emission in PIXE or SEM-EDS systems is described by a Poisson distribution (Goldstein et al., 1981), analytic uncertainties ($\sigma_{Ti, Ca, K}$ and σ_{CR}) decrease as a function of the square root of dwell time. Analyses reported in this paper were made by increasing SEM dwell time from the standard 40 s to 4000–6000 s; this change increased measurement precision by a factor greater than three. High-precision analyses are critical for determining the actual variability of varnish chemistry, variability that in the past was masked by less-precise analyses.

Analytic Precision Limits the Certainty of Cation-Ratio Ages

The precision with which each cation ratio is determined limits the certainty of the sample

mean cation ratio, \overline{CR} , and therefore the age calculated for any geomorphic surface according to the standard error of the mean,

$$\sigma_{\mu_{CR}} = n^{-0.5} \overline{\sigma}_{CR} \quad (2)$$

We use equations 1 and 2 to adjust dwell time and/or determine the number of analyses of a single sample necessary to determine the cation ratio for that sample with a specific precision. However, equations 1 and 2 can also be used to calculate the maximum precision with which \overline{CR} can be determined by a given analytic technique and/or number of analyses.

For example, if the analyzed samples are chemically identical (e.g., aliquots of homogenized varnish) and if errors in Ti, Ca, and K are uncorrelated, the sample standard deviation, S_{CR} , of \overline{CR} should approximately equal σ_{CR} as determined by equation 1 (see Fig. 1). However, the actual uncertainty of CR is determined by equation 2, which accounts for the number of analyses used to calculate the mean. Because varnish samples collected from different boulders are not chemically identical, S_{CR} for multiple boulders on a single geomorphic surface should exceed σ_{CR} .

Data reported by Nobbs and Dorn (1988) are inconsistent because the "standard errors" (S_{CR}) for the mean of chemically heterogeneous varnish samples are only 2%–3%, despite cation-ratio uncertainties (σ_{CR}) of 8%–12% (see comment by Harrington and Reneau *in* Nobbs and Dorn, 1988). This inconsistency is even more striking because the reported σ_{CR} reflects only σ_{Ti} without considering σ_K and σ_{Ca} (R. I. Dorn, 1990, personal commun.).

We resolved the inconsistency in data of

Nobbs and Dorn by preparing and analyzing glass analogs of rock varnish. We analyzed 15 samples (5 homogeneous aliquots from each of 3 different synthetic varnishes) by PIXE UCD. Table 1 shows that sample standard deviations for three sets of five independent measurements of Ti, Ca, and K range from 5% to 11%; however, sample standard deviations for cation ratios calculated from these analyses are only 2% to 4%, lower by a factor of two or three than the uncertainty calculated by Nobbs and Dorn or predicted by error propagation (equation 1). Our measurements indicate that uncertainties reported by Nobbs and Dorn (1988) for individual cation-ratio determinations are inaccurate because they did not recognize that errors in Ti, Ca, and K analyses were correlated.

Synthetic varnish analyses suggest that the actual precision (σ_{CR}) of PIXE UCD cation-ratio analyses is 2%–4%. Nobbs and Dorn (1988) and Dorn et al. (1987) reported an average S_{CR} of 2.7% ($n = 24$) and 2.9% ($n = 8$), respectively. Because these values of $S_{CR} \approx \sigma_{CR}$, samples analyzed by Dorn are chemically homogeneous. Harrington and Whitney (1987) reported $S_{CR} \geq \sigma_{CR}$, a finding consistent with chemically heterogeneous varnish.

Representative Method for Expressing the Uncertainty of the Mean Cation Ratio

A varnish sampling program, no matter how well designed, only estimates μ_{CR} of a varnish population. Because most of the varnish population has not been sampled, any \overline{CR} will always have some uncertainty; however, the magnitude of this uncertainty can be reduced by analyzing more samples from the varnish population.

Dorn et al. (1987) and Harrington and Whit-

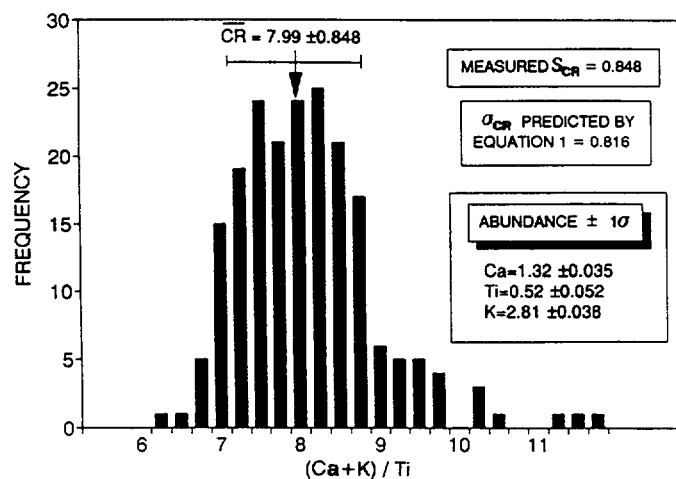


Figure 1. Replicate analyses ($n = 200$; rastered area = 6 mm^2 ; $\sigma_{CR} \sim 10\%$ by equation 1) of same patch of varnish give wide range of cation ratios ($S_{CR} \sim 10.5\%$) as predicted by equation 1 (sample BT-2, Bishop Tuff). Similarity of S_{CR} and σ_{CR} indicates equation 1 correctly predicts uncertainty of a SEM-EDS CR analysis.

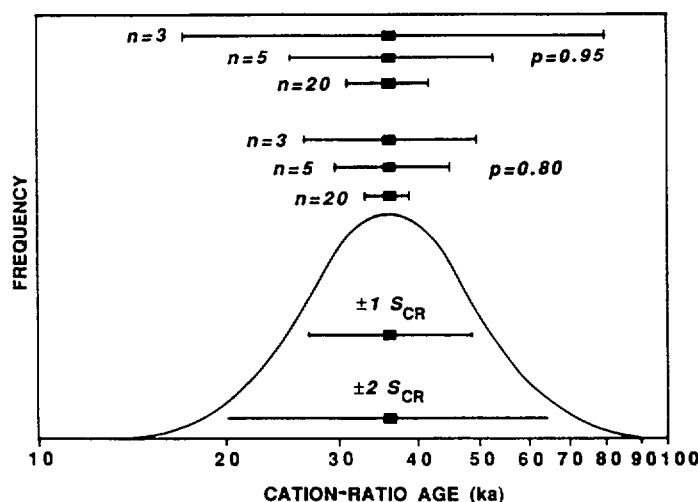


Figure 2. Normally distributed cation-ratio population with $\overline{CR} = 4.5$ and $S_{CR} = 5\%$. Confidence intervals (equation 3) about CR are shown for various probabilities p and numbers of samples n . Confidence intervals expressed as ages by using $a = 10^{[(13.12 - CR)/1.89]}$ (Dorn et al., 1987). One and two standard deviations (S_{CR}) of cation-ratio population are also plotted.

ney (1987) characterized the uncertainty in \overline{CR} and the associated age by reporting only the standard deviation, S_{CR} , of the cation ratios used to estimate \overline{CR} without explicitly stating n . This approach is inappropriate because S_{CR} only describes the population of cation ratios from which samples were taken; alone, S_{CR} does not accurately indicate the uncertainty with which \overline{CR} has been determined. The uncertainty in \overline{CR} can be quantified by using a confidence interval that takes into account the number of analyses used to estimate \overline{CR} :

$$\begin{aligned} (\overline{CR} - [t_{\alpha/2} S_{CR} n^{-0.5}]) < \mu_{CR} \\ < (\overline{CR} + [t_{\alpha/2} S_{CR} n^{-0.5}]), \end{aligned} \quad (3)$$

and

$$\sigma' = 100(t_{\alpha/2} S_{CR} n^{-0.5} \overline{CR}^{-1}). \quad (4)$$

Equation 3 indicates the interval within which there is a $(1 - \alpha)$ probability that the true mean cation ratio μ_{CR} for the sampled population is contained. Equation 4 expresses this interval in terms of σ' , a percentage of \overline{CR} . We refer to σ' as the fractional uncertainty of \overline{CR} .

Because the number of samples used to determine \overline{CR} is usually small ($n < 30$), it is appropriate to calculate confidence intervals with the Student's t probability distribution, $t_{\alpha/2}$ (Freund, 1988). The magnitude of $t_{\alpha/2}$ is inversely proportional to n and is especially large when $n \leq 5$ and $p \geq 0.9$. This relation quantifies the common-sense conclusion that the \overline{CR} for a geomorphic surface will be more reliably determined if a large number of samples from that surface are analyzed. Values of $t_{\alpha/2}$ may be found in Freund (1988).

An example (Fig. 2) illustrates the usefulness of equations 3 and 4. If three cation ratios were averaged to determine a \overline{CR} with $S_{CR} = 5\%$, the

fractional uncertainty σ' of the \overline{CR} at 0.95 probability would be about 12.5%. In this case, reporting the uncertainty as two standard deviations ($2S_{CR}$), approximately equivalent to $p = 0.95$, would underestimate the uncertainty in \overline{CR} (10% vs. 12.5%). However, if 20 rather than 3 cation ratios were averaged to determine \overline{CR} , σ' would be about 2.5%. In this case, reporting the uncertainty as $2S_{CR}$ would overestimate the uncertainty in \overline{CR} by a factor of four (10% vs. 2.5%).

The uncertainty of \overline{CR} is predicted most accurately by equations 3 and 4 if the cation-ratio population from which samples are drawn is normally distributed. Because cation-ratio data do not always satisfy formal criteria for normality, confidence intervals calculated for \overline{CR} for using equations 3 and 4 will be approximate.

Scale of Variance in Rock-Varnish Chemistry

If varnish could be sampled so as to reduce S_{CR} , \overline{CR} would be determined more precisely (equations 3 and 4). Our measurements show that S_{CR} increases as the area of varnish included in a single analysis decreases (Fig. 3), although \overline{CR} changes only slightly. Due to the patchy nature of varnish coatings in Owens Valley, we could not extend these measurements to areas larger than $\sim 6 \text{ mm}^2$. However, S_{CR} will again increase when the sampled area becomes large enough to include multiple populations of cation ratios; e.g., when varnish is inadvertently sampled across the edge of an ancient fire spall.

The scale at which varnish heterogeneity begins to increase has yet to be determined and probably varies with the exposure age and weathering characteristics of the underlying rock. We anticipate that varnish areas of about 10 cm^2 and larger (the average size of fire spalls) may contain multiple cation-ratio populations. If \overline{CR} is determined by analyzing areas of var-

nish small enough to avoid sampling multiple populations, cation-ratio homogeneity can be examined and significantly different chemistry (i.e., different varnish populations) can be recognized (C. Harrington, 1990, personal commun.). Knowing the scale of variability is important because, if leaching assumptions of Dorn (1989) are correct, μ_{CR} will not be a valid indicator of exposure age if multiple cation-ratio populations (i.e., varnish of different ages) are combined in a single chemical analysis.

TWO EXAMPLES OF CATION-RATIO PRECISION

Data from Owens Valley and statistical deductions illustrate the potential temporal resolution of varnish cation ratios. In Figure 4, cation ratios are expressed as age ranges calculated from a calibration determined empirically for Owens Valley cation-ratio dating by Dorn et al. (1987). The calculations show that moraines and alluvial fans from marine oxygen-isotope stages 2, 4, and 6 (ca. 10–200 ka) should be separable by means of cation-ratio data, provided cation ratios change predictably with time and provided \overline{CR} can be determined with $\sigma' \leq 10\%$ (Fig. 4A). By comparison, discrimination of surfaces exposed during Holocene neotectonic events requires that \overline{CR} be determined with a much smaller σ' , $\leq 3\%$ (Fig. 4B). Obtaining the small σ' values necessary to resolve closely spaced events would require numerous analyses of varnish (large n and small $t_{\alpha/2}$), sampling an area of varnish that minimizes cation-ratio variance (small S_{CR}), and acceptance of a lower probability (small $t_{\alpha/2}$).

Using equation 4, we can estimate the probability with which geologic events might be separated by using cation ratios. For example, the smallest S_{CR} we determined on a 5 cm^2 varnish sample was about 5% of \overline{CR} (Fig. 3). If the \overline{CR}

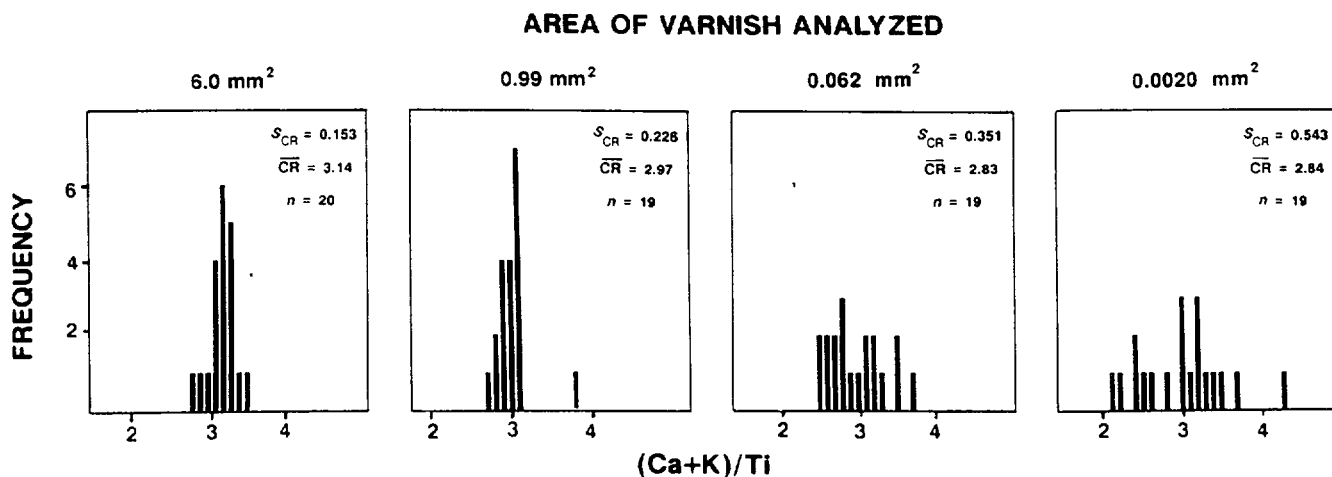
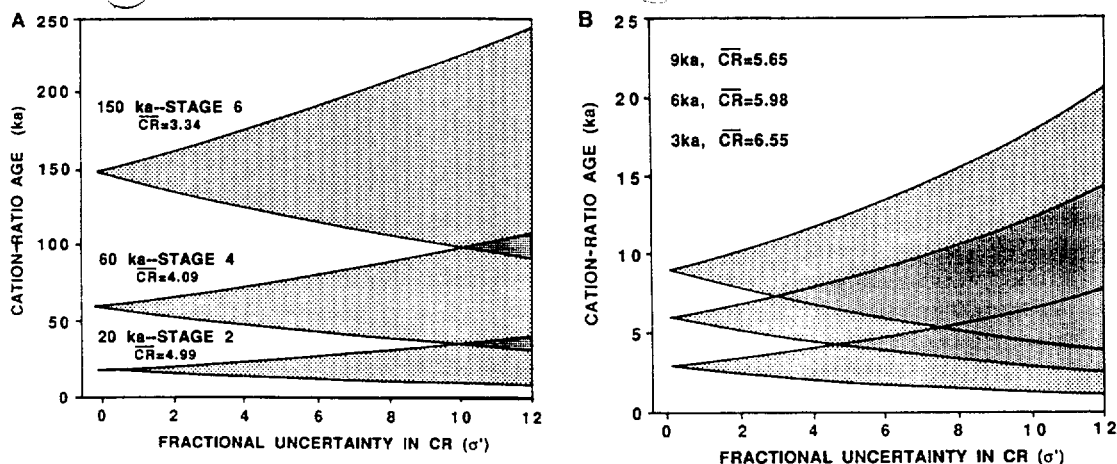


Figure 3. Variance of varnish chemistry and, therefore, S_{CR} increase as area of varnish included in each analysis decreases. Data were collected by using SEM-EDS and acquisition times of 4000–6000 s, sufficient to determine each cation ratio with $\sigma_{CR} < 1\%$. Sample FS-2, Fish Springs cinder cone.

Figure 4. Age ranges calculated by using $a = 10^{((13.12 - CR)/1.89)}$ (Dorn et al., 1987) after adding and subtracting arbitrary σ' from CR. If calculated age ranges overlap (dark stipple), events are not separable at arbitrary value of σ' . Note that actual σ' associated with any reported CR can be calculated by using equation 4 and varies with n , $t_{\alpha/2}$ and S_{CR} . **A:** Late Pleistocene glacial deposits in Sierra Nevada are separable if $\sigma' \leq 10\%$. **B:** Holocene neotectonic events require $\sigma' \leq 3\%$ to be separable.



and S_{CR} of this single disk are representative of the geomorphic surface from which it was collected and if five or more analyses made on this disk are used to estimate \overline{CR} , then glaciations ($\sigma' \leq 10\%$) will be separable with more than 95% probability and neotectonic events ($\sigma' \leq 3\%$) will be separable with almost 80% probability. This calculation assumes that cation ratios change continuously with time and that each cation-ratio determination is precise ($\sigma_{CR} \leq 2\%$ if $n = 5$). If cation-ratio analyses are less precise, the cation-ratio population more heterogeneous, or a greater level of confidence is required, more samples from the population must be analyzed to achieve a similar σ' .

The temporal separability shown by these calculations suggests that cation ratios may be useful for the relative dating and correlation of landforms. However, if numerical cation-ratio ages are generated using a calibration curve, then the accuracy and precision of cation-ratio calibration must also be considered rigorously before cation-ratio ages can be compared to ages generated by other dating methods.

CONCLUSIONS

The maximum precision with which a mean cation ratio of rock varnish can be determined and the minimum uncertainty in the age calculated from that cation ratio are proportional to the precision of the method used to determine the ratio and inversely proportional to the number of samples analyzed.

The uncertainty of a measured mean cation ratio and of the age calculated from that mean cation ratio depend strongly on the number of samples used to estimate the mean. Therefore, uncertainty in a cation-ratio age should be calculated from the expected variation (equations 3 and 4) of the mean cation ratio rather than the standard deviation of the cation-ratio determinations used to calculate the mean.

The variance of varnish chemistry decreases as larger areas of varnish are sampled, at least up

to a sample area of 6 mm^2 . However, if cation leaching occurs and if too large an area of varnish is included in each analysis, variance will again increase as multiple cation-ratio populations are included in single samples.

APPENDIX 1. NOMENCLATURE

n	Number of independent chemical analyses or cation-ratio determinations
Ca, K, Ti	Analytic abundance (elemental wt%)
CR	Cation ratio, $(K + Ca)/Ti$, of varnish
\overline{CR}	Arithmetic mean of n cation-ratio determinations (sample mean)
$\sigma_{Ti,Ca,K}$	Analytic uncertainty of a single abundance measurement (one standard deviation) (elemental wt%)
σ_{CR}	Analytic uncertainty of a single cation-ratio determination (one standard deviation)
$\sigma_{\mu_{CR}}$	One standard error of the mean cation ratio (n cation-ratio determinations)
$\overline{\sigma}_{CR}$	Average analytic uncertainty of n cation-ratio determinations (one standard deviation)
S_{CR}	Sample standard deviation of n cation ratios used to determine CR
σ'	Fractional uncertainty of n cation ratios (%)
μ_{CR}	Population mean cation ratio
p	Probability $(1 - \alpha)$
$t_{\alpha/2}$	Student's t value at $(n - 1)$ degrees of freedom and $(1 - \alpha)$ probability
a	Age (yr)
α	$(1 - p)$ value of probability

REFERENCES CITED

- Bailey, R.A., Dalrymple, G.B., and Lanphere, M.A., 1976, Volcanism, structure and geochronology of Long Valley Caldera, Mono County, CA: *Journal of Geophysical Research*, v. 81, p. 725-744.
- Bard, J.C., 1979, The development of a patination dating technique for Great Basin petroglyphs using neutron activation and X-ray fluorescence analysis [Ph.D. thesis]: Berkeley, University of California, 409 p.
- Dorn, R.I., 1983, Cation-ratio dating: A new rock varnish age-determination technique: *Quaternary Research*, v. 20, p. 49-73.
- 1989, Cation-ratio dating of rock varnish: A geographic assessment: *Physical Geography*, v. 13, p. 559-596.
- Dorn, R.I., and Oberlander, T.M., 1982, Rock varnish: Progress in *Physical Geography*, v. 6, p. 317-367.

- Dorn, R.I., Turrin, B.D., Jull, A.J., Linick, T.W., and Donahue, D.J., 1987, Radiocarbon and cation-ratio ages for rock varnish on Tioga and Tahoe morainal boulders of Pine Creek, eastern Sierra Nevada, California, and their paleoclimatic implications: *Quaternary Research*, v. 28, p. 38-49.
- Dragovich, D., 1988, A preliminary electron probe study of microchemical variations in desert varnish in western New South Wales, Australia: *Earth Surface Processes and Landforms*, v. 13, p. 259-270.
- Freund, J.E., 1988, *Modern elementary statistics*: Englewood Cliffs, New Jersey, Prentice-Hall, 574 p.
- Goldstein, J.I., Newbury, D.E., Echlin, P., Joy, D.C., Fiori, C., and Lifshin, E., 1981, *Scanning electron microscopy and X-ray microanalysis*: New York, Plenum Press, 673 p.
- Harden, J.W., Reheis, M.C., Sowers, J.M., and Slate, J.L., 1988, Comment on "Scanning electron microscope method for rock varnish dating": *Geology*, v. 16, p. 1051.
- Harrington, C.D., and Whitney, J.W., 1987, Scanning electron microscope method for rock varnish dating: *Geology*, v. 15, p. 967-970.
- Martel, S.J., Harrison, T.M., and Gillespie, A.R., 1987, Late Quaternary vertical displacement rate across the Fish Springs fault, Owens Valley fault zone, California: *Quaternary Research*, v. 27, p. 113-129.
- Nobbs, M., and Dorn, R.I., 1988, Age determinations for rock varnish formation with petroglyphs: Cation-ratio dating of 24 motifs from the Olary region of arid South Australia: *Rock Art Research*, p. 108-146.

ACKNOWLEDGMENTS

Supported by American Association of Petroleum Geologists and University of Washington grants to Bierman and U.S. Geological Survey NEHRP Grant 14-08-0001-G1783 to Gillespie and Bierman. We thank K. Campbell, S. Reneau, S. Porter, M. Ghiorso, C. Harrington, L. McFadden, and D. Clark for their reviews, and B. Atwater for particularly insightful commentary. We also thank F. Bardsley for help in manuscript preparation.

Manuscript received June 5, 1990
 Revised manuscript received August 29, 1990
 Manuscript accepted September 7, 1990

Southeast Australian late Mesozoic and Cenozoic denudation rates: A test for late Tertiary increases in continental denudation

Paul Bishop

Department of Geography, University of Sydney, Sydney, New South Wales 2006, Australia

ABSTRACT

Throughout the Tertiary, average rates of erosion of southeast Australia have been uniformly low (about 10^{-3} mm/yr of surface lowering), indicating that this part of the Australian continent did not contribute to a rapid increase in ocean-basin sedimentation over the past 15 or 20 m.y. Somewhat higher Mesozoic rates may be the result of minor tectonism, but explanation for the generally low Cenozoic and Mesozoic erosion rates may be sought in the forest cover and general tectonic stability of southeast Australia over this time period. Australia's gradually increasing aridity/climatic seasonality over the past 20 m.y. has apparently not resulted in higher average rates of erosion of the continent, except perhaps in the very latest Tertiary and Quaternary.

INTRODUCTION

Compilation of rates of world ocean sedimentation (Davies et al., 1977) indicated an abrupt, order of magnitude increase in sedimentation at 20 Ma. Donnelly (1982) identified an abrupt increase in ocean sedimentation about 15 Ma. and arguing like Davies et al. (1977) that the increases were largely independent of geographic location, he ascribed the higher rates to increased continental denudation in the late Tertiary as the result of increasing climatic variability over the time interval. On the basis of the present low erosion rates of semiarid Australia, Davies et al. (1977) argued the opposite, that the late Tertiary increase in ocean-basin sedimentation resulted from higher rates of continental denudation under increased rainfall.

Neither study presented data from studies of Tertiary continental history to test the attribution of increased oceanic sedimentation to worldwide increased continental denudation as a result of climatic change. Moreover, the geographically more specific data of Donnelly (1982, Fig. 1) indicated, as he noted, that the increase in ocean-basin sedimentation was not fully global in extent. The ocean basins that receive sediment only from the Australian mainland apparently did not experience the late Tertiary increase in sedimentation, a variation that Donnelly (1982) explained in terms of sedimentary complications accompanying fragmentation of Gondwanan continents.

This paper (1) reports average rates of denudation of southeast Australia for various time intervals from the Mesozoic to the present to test for increased late Tertiary continental denudation; (2) compares the southeast Australian denudation rates over time with the region's climatic history; and (3) tests, by implication from 1, whether low oceanic sedimentation rates off Australia are matched by low rates of continental denudation, a central point in the cases argued by Davies et al. (1977) and Donnelly (1982).

STUDY AREA AND METHODS

Erosion rates were determined for the Murray-Darling drainage systems (10^6 km²—the largest river system in Australia) at areal scales

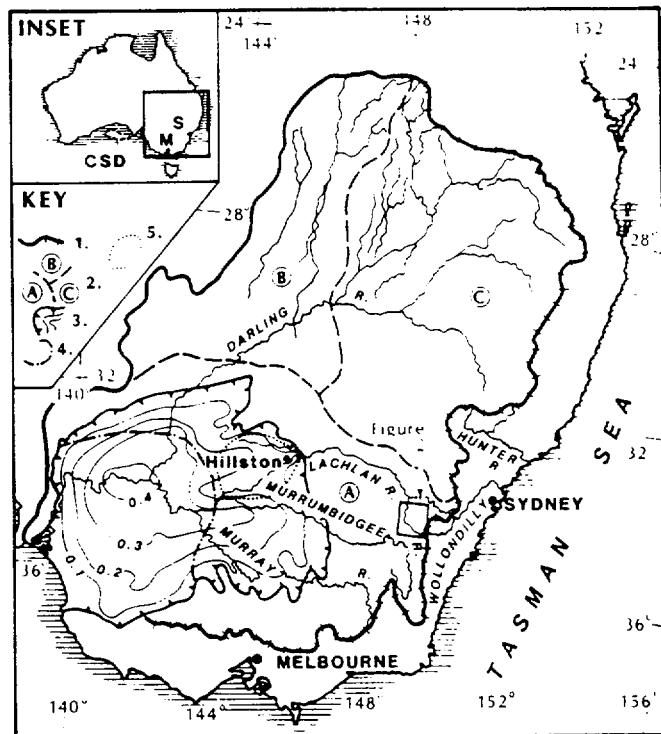


Figure 1. Southeast Australia showing Murray-Darling catchment and some other major rivers; 1 = boundary of Murray-Darling catchment; tick marks indicate where boundary is Australian continental drainage divide; 2 = subcatchment boundaries within Murray-Darling catchment; 3 = Murray Basin boundary and isopachs (km) of total Cenozoic sediment thickness; 4 = limit of Miocene marine transgression; 5 = Lachlan fan. Inset shows Australian continent and locations of main figure and Ceduna Saddle depocenter (CSD); M = Melbourne; S = Sydney.

ranging from the headwaters of one of the major tributaries, the upper Lachlan, southwest of Sydney, to the whole catchment (Figs. 1, 2). The Murray-Darling drains from the crest and western flanks of the southeast Australian highlands (<2 km above sea level) to the Southern Ocean via the Murray Basin, an intracratonic basin having a thin fill (<0.5 km) of mixed marine and terrestrial sediments spanning most of the Cenozoic (Macumber, 1978; Woolley, 1978).

Rates of erosion have been determined from rates of river incision below radiometrically dated, valley-filling basaltic lavas, rates of sedimentation in sedimentary basins, and rates of denudation necessary to expose granites containing apatites having known fission-track ages. Eolian erosion is thought to be unimportant because the vegetation cover of the study area was closed forest for most of the late Mesozoic and Cenozoic

(see below). The role of chemical erosion is unclear but is ignored, with the caveat that the absolute rates may have to be revised upward if chemical erosion is ultimately shown to be significant over this time interval in this area. The differences between the various rates of erosion, nonetheless, would still remain largely the same.

TERTIARY EROSION RATES IN THE UPPER LACHLAN

In the upper Lachlan valley, New South Wales (Fig. 2), radiometrically dated early Miocene and early Eocene basalts, all overlying cross-bedded, fluvial sands and gravels, mark former channels of the Lachlan River and its tributaries (Wellman and McDougall, 1974; Young and Bishop, 1980). Average rates of post-early Miocene incision were determined by dividing the height difference between the present channel of the Lachlan River and the top of adjacent basalt remnants by the age of the basalt (20–21 Ma; Fig. 2). This gives a minimum rate of postbasalt

incision, because of posteruption erosional loss of some of the upper parts of the lava flows, but such losses are certainly not sufficient to alter the rate of incision at the order of magnitude level (Bishop, 1984). This post-20-Ma rate of incision is 0.008 mm/yr.

Rates of incision between the early Eocene and the early Miocene can be determined on the same basis, using the height difference between the base and top, respectively, of adjacent basalts of these two ages, 16 km west of Crookwell (Fig. 2). Erosional losses from the upper surface of the Eocene basalt are potentially much higher, given its greater age; therefore, the incision rate for the period early Eocene to early Miocene is likely to be underestimated by a greater amount than is the case with the post-early Miocene rate. Further underestimation arises from the distance of this site from the main channel of the Lachlan and the observed headward decline in river incision during the Tertiary (Bishop, 1984). The calculated rate is 0.003 to 0.004 mm/yr.

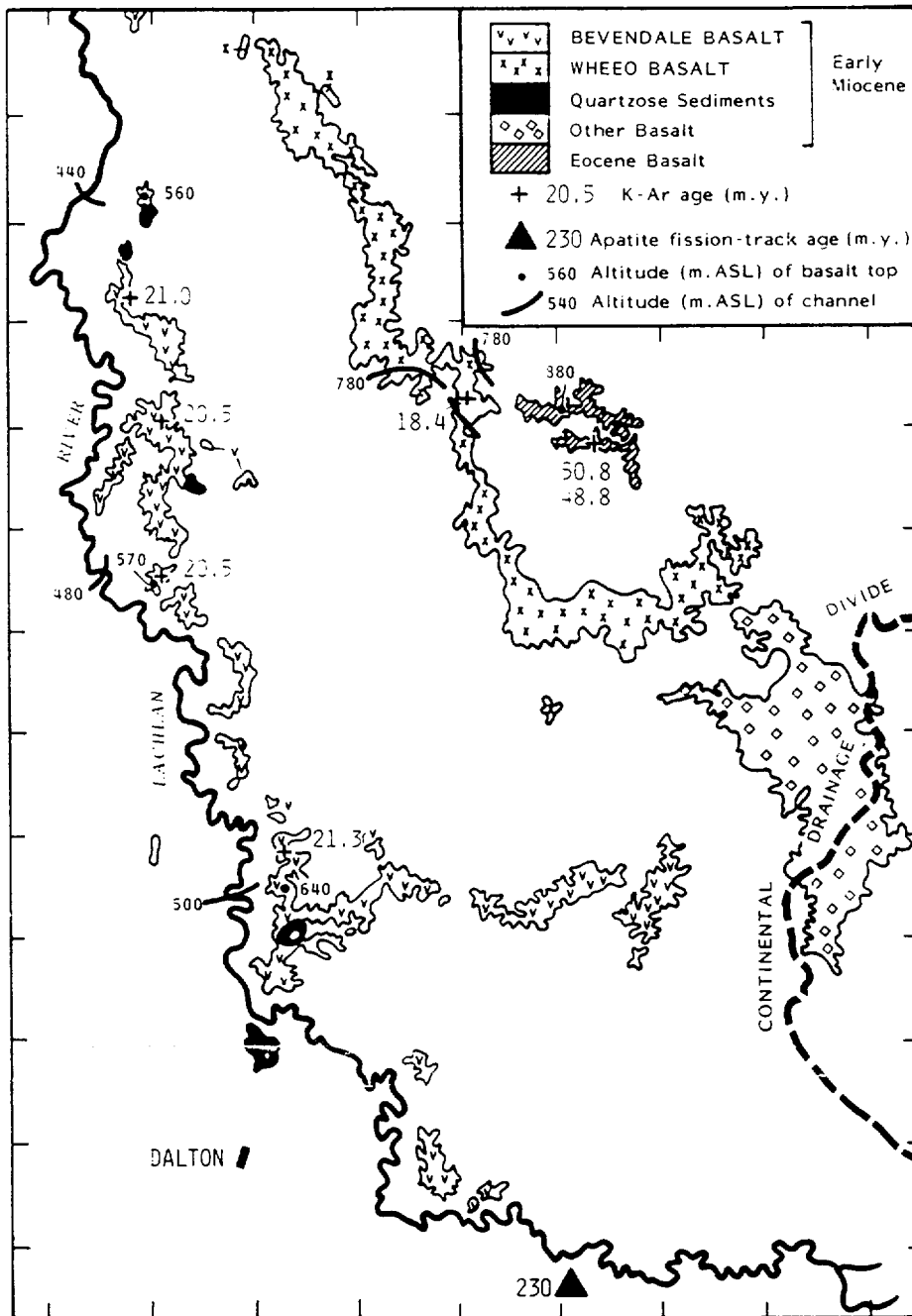


Figure 2. Upper Lachlan valley showing principal features of Tertiary geology and location of one of apatite fission-track ages discussed in text. Locality of second fission-track age determination in upper Lachlan is 30 km north-northeast of Eocene K-Ar dating locality. Tick marks around border are on Australian Map Grid at 4000-m intervals.

LATE CENOZOIC RATE OF SEDIMENT SUPPLY BY THE LACHLAN

The post-Oligocene rate of denudation of the Lachlan catchment upstream of the Murray Basin may also be determined from the volume of sediment in the Lachlan's upland valley and in the wedge of sediment deposited in the Murray Basin by the Lachlan River between Hillston and the Murrumbidgee River. This sediment is essentially uncompacted (Brown, 1983) and for the purposes of determining denudation rates is treated as being derived directly from the erosion of bedrock (assumed densities: sediment 1.5, bedrock 2.65). Sediment volumes were computed from published depths to basement (Martin, 1973; Woolley, 1978), and the ages of the basal sediments in both the fan and the upland valley were found to be not greater than late Oligocene-early Miocene, on the basis of their palynological content (Martin, 1973, 1977; Woolley, 1978). Breaks in sedimentation are not included in these computations because breaks in incision in the upper Lachlan cannot be determined.

The rate of catchment erosion necessary to provide the volumes of sediment will be a minimum, in this case because of sediment bypassing the Lachlan fan depositional site. However, the presence of marine authigenic sediment almost to the Lachlan-Murrumbidgee confluence for 45% to 55% of the past 25 m.y. (Woolley, 1978) means that the bulk of sediment eroded from the bedrock valley of the Lachlan above Hillston since the Oligocene was probably deposited upstream of the Murrumbidgee. The various quantities imply a rate of catchment erosion of 0.004 mm/yr for the past 25 m.y.

TERTIARY DENUDATION OF THE MURRAY-DARLING

An average rate of denudation of the Murray-Darling system throughout the Tertiary can be determined from the volume of terrigenous sediment in the Murray Basin. Isopachs of total Cenozoic sediment thickness in the basin (Australian Bureau of Mineral Resources, 1979) give the total volume of basin sediment from which was subtracted the volume of authigenic sediment (limestone), computed using the areal extent of the major marine transgression (Miocene; Fig. 1) and thickness of this limestone (Woolley, 1978).

The terrigenous sediment was probably derived largely from the higher relief catchment areas to the immediate south, east, and, to a lesser degree, north of the Murray Basin (i.e., subcatchment A in Fig. 1), and perhaps there were lower inputs from the very low gradient streams draining the lower relief areas farther north (subcatchment B). Subcatchment C has probably not delivered much sediment to the Murray Basin but has largely been the source of sediments in the Darling Basin, a late Mesozoic and Cenozoic depositional site northeast of the Murray Basin (Taylor, 1978; Australian Bureau of Mineral Resources, 1979).

The sediment volumes and catchment relationships indicate average rates of erosion throughout the Tertiary of 0.003 mm/yr in the most likely case of the sediment being derived largely from subcatchment A, or 0.001 mm/yr if the source area was the combined areas of subcatchments A and B.

LATE CRETACEOUS AND POST-PERMIAN DENUDATION

An estimate of the average rate of Late Cretaceous denudation of the whole of the highlands western flank may be made on the basis of the quantity of sediment in the Ceduna Saddle depocenter in the Great Australian Bight (Fig. 1). Veevers (1982) suggested that the bulk of the $0.5 \times 10^6 \text{ km}^3$ of sediment (say, $0.4 \times 10^6 \text{ km}^3$) deposited during the post-Cenomanian Late Cretaceous in the Ceduna Saddle came from the eastern highlands via an ancient Murray-Darling drainage system. If this Ceduna Saddle sediment was derived from a Murray-Darling drainage system of dimensions similar to those of the present, the average rate of highland erosion in the 25 m.y. of the post-Cenomanian Late Cretaceous is estimated to range from 0.013 mm/yr if the sediment was derived

from the full catchment (i.e., subcatchments A, B, and C) to 0.047 mm/yr in the more probable case of the sediment being derived largely from subcatchment A.

The average post-Permian denudation rate can be computed from 230 Ma and 235 Ma apatite fission-track ages from upper Lachlan granitoids (Fig. 2) (Morley et al., 1981). The fission tracks date from when the granites last passed below $100 \pm 20 \text{ }^\circ\text{C}$. The depth at which the temperature passed below about $100 \text{ }^\circ\text{C}$ depends on the geothermal gradient, which is currently high in southeast New South Wales ($25\text{--}30 \text{ }^\circ\text{C}/\text{km}$; Cull, 1979; Morley et al., 1981). The geothermal gradient has been high since the Mesozoic, at least, and possibly since the Permian (Ferguson et al., 1979; Middleton and Schmidt, 1982; Wass and Hollis, 1983; Griffin et al., 1984). A geothermal gradient of $30 \text{ }^\circ\text{C}/\text{km}$ is therefore assumed for 200 to 230 Ma, implying 3.3 km of surface lowering in the upper Lachlan since 230 Ma, at an average rate of denudation of 0.014 mm/yr. A higher geothermal gradient of $50 \text{ }^\circ\text{C}/\text{km}$ (Middleton and Schmidt, 1982) is not unreasonable for the relatively short times needed to reset fission tracks, and this would result in a denudation rate of 0.009 mm/yr.

DISCUSSION

Average rates of incision and denudation for the Murray-Darling system (Fig. 3) have been uniformly low ($<10^{-2} \text{ mm}/\text{yr}$) over the Cenozoic and somewhat higher in the Mesozoic. An order of magnitude increase in erosion rates certainly did not occur at 20 Ma: the apparent doubling of the rate in the upper Lachlan at 20 Ma merely reflected erosional losses from the upper surface of early Eocene basalts and the site's upstream distance from the trunk stream. An increase in erosion probably did not occur at 15 Ma either, given that such an increase would be expected to show up in a higher average post-20-Ma rate.

Other studies of rates of postbasalt incision of both the western and eastern flanks of the highlands of southeast Australia (cf. Wellman, 1979;

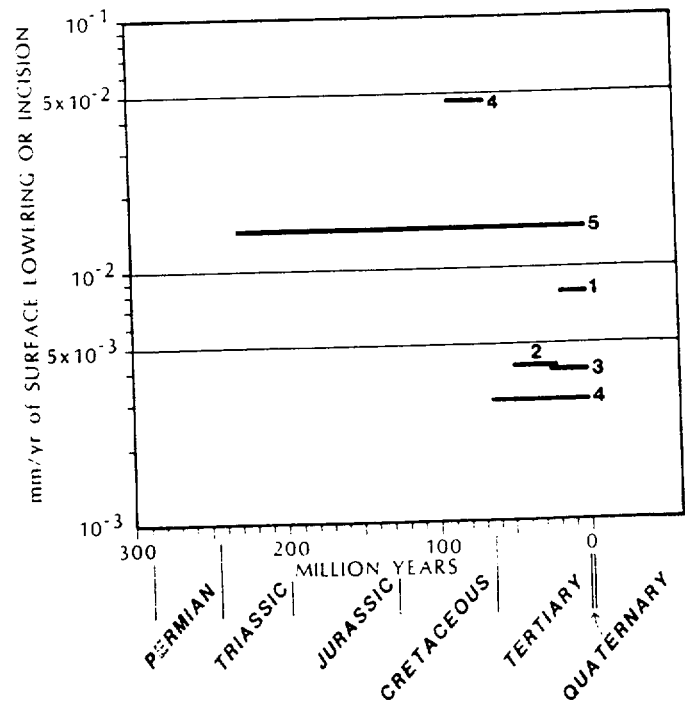


Figure 3. Summary of rates of incision and denudation from Murray-Darling catchment; methods of determination are indicated by numbers: 1 = postbasalt incision; 2 = river incision between basalts of two ages; 3 = fan sedimentation; 4 = basin sedimentation; 5 = exposure of granitic rocks containing apatites having known fission-track ages.

Young, 1983) confirm both the low magnitudes and the general uniformity of the Cenozoic erosion rates reported here. Wellman's (1979) uplift model for these highlands is based on constant rates of river incision, at least for the past 45 m.y. Wellman's Figure 3 suggested, however, that relief rather than uniform uplift is the more important control of rates of river incision, an observation in keeping with data from elsewhere (Ruxton and McDougall, 1967; Ahnert, 1970).

Such variations in local relief can be the result of prior tectonic history. Stephenson and Lambeck (1985) argued that the present highlands are the remnants of a Paleozoic highland belt that has experienced no dynamic tectonism since the Paleozoic. Isostatic rebound in compensation for erosion has been the only vertical movement of the highlands in that time, and this rebound has become increasingly significant during the Cenozoic. This study's somewhat higher Mesozoic erosion rates in comparison with the Cenozoic rates reflect these progressive declines in relief and incision due to isostatic rebound.

The data presented here and by others (Wellman, 1979; Young, 1983) indicate, therefore, that the Australian continent has not contributed to the observed increase in oceanic sedimentation in the late Tertiary. The data also confirm that low continental denudation rates are matched by low rates of oceanic sedimentation, given the low post-20-Ma rates of sedimentation of the ocean south of Australia reported by Donnelly (1982). It is apparent, therefore, that the Australian mainland did not experience abruptly increased erosion 15–20 m.y. ago; it is also clear from plant microfossil and macrofossil evidence that the southeastern Australian climate experienced gradually increasing seasonality and aridity during the Tertiary (Bowler, 1976, 1982). This general change seems not to have been associated with increased sediment yields, however, because initially the vegetation apparently changed from temperate, closed rain forest dominated by *Nothofagus* sp. to closed Myrtaceae-Casuarine forest that seems to have maintained the relatively low average rates of erosion reported here. Only in the very latest Tertiary and Quaternary in southeast Australia did these forests break up in response to an increasingly arid and seasonal climate, to be replaced by discontinuous forest and grasslands (Kemp, 1978; Martin, 1981). This final, relatively recent breakup of the forests may have been accompanied by increased rates of erosion that have not shown up in the average rates presented here, much in the way envisaged by Taylor (1978) for the upper Darling Basin.

CONCLUSIONS

Donnelly's (1982) Tertiary climatic deterioration occurred in Australia, but it was neither as abrupt nor as early in the Tertiary as Donnelly suggested. The Australian continent has apparently not experienced the dramatic increase in rates of continental denudation in the middle to late Tertiary. Rather, the Australian data suggest that the Cenozoic erosion rates have been uniformly low in response to minimal tectonic activity and closed forest cover.

The increases in oceanic sedimentation are not independent of geographic location, as noted by Donnelly (1982), and that Australia has indeed experienced a climatic deterioration but maintained the low rates of erosion, at least for part of its duration, suggests that nonclimatic factors may be of more significance than Davies et al. (1977) acknowledged in explaining late Tertiary increases in oceanic sedimentation.

REFERENCES CITED

Ahnert, F., 1970. Functional relationships between denudation, relief, and uplift in large mid-latitude drainage basins: *American Journal of Science*, v. 268, p. 243–263.

Australian Bureau of Mineral Resources, 1979. *Earth science atlas*: Canberra, Australia.

Bishop, P., 1984. *Stability or change: The Late Cainozoic history of the Wollondilly and Upper Lachlan Rivers* (Ph.D. thesis): North Ryde, New South Wales, Macquarie University, 165 p.

Bowler, J.M., 1976. Aridity in Australia: Age, origins and expression in aeolian landforms and sediments: *Earth Science Reviews*, v. 12, p. 279–310.

— 1982. Aridity in the late Tertiary and Quaternary of Australia. *in* Barker, W.R., and Greenslade, P.J.M., eds., *Evolution of the flora and fauna of arid Australia*: Frewville, South Australia. Peacock Publications, p. 35–45.

Brown, C.M., 1983. Discussion of "A Cainozoic history of Australia's Southeast Highlands": *Geological Society of Australia Journal*, v. 30, p. 483–486.

Cul, J.P., 1979. Heat flow and geothermal energy prospects in the Otway Basin, SE Australia: *Search*, v. 10, p. 429–433.

Davies, T.A., Hay, W.W., Sentham, J.R., and Worsley, T.R., 1977. Estimates of Cenozoic oceanic sedimentation rates: *Science*, v. 197, p. 53–55.

Donnelly, T.W., 1982. Worldwide continental denudation and climatic deterioration during the late Tertiary: Evidence from deep-sea sediments: *Geology*, v. 10, p. 451–454.

Ferguson, J., Arculus, R.J., and Joyce, J., 1979. Kimberlite and kimberlitic intrusives of southeastern Australia: A review: *Bureau of Mineral Resources Journal of Australian Geology and Geophysics*, v. 4, p. 227–241.

Griffin, W.L., Wass, S.Y., and Hollis, J.D., 1984. Ultramafic xenoliths from Bullenmerri and Gnotuk maars, Victoria, Australia: Petrology of a sub-continental crust–mantle transition: *Journal of Petrology*, v. 25, p. 53–87.

Kemp, E.M., 1978. Tertiary climatic evolution and vegetation history in the southeast Indian Ocean region: *Palaeogeography, Palaeoclimatology, Palaeoecology*, v. 24, p. 169–208.

Macumber, P.G., 1978. Evolution of the Murray River during the Tertiary Period. Evidence from northern Victoria: *Royal Society of Victoria Proceedings*, v. 90, p. 43–52.

Martin, H.A., 1973. Upper Tertiary palynology in southern New South Wales: *Geological Society of Australia Special Publication* 4, p. 35–54.

— 1977. The Tertiary stratigraphic palynology of the Murray Basin in New South Wales. 1. The Hay-Balranald-Wakool districts: *Royal Society of New South Wales Journal and Proceedings*, v. 110, p. 41–47.

— 1981. The Tertiary flora, *in* Keast, A., ed., *Ecological biogeography of Australia*: The Hague, W. Junk, p. 391–406.

Middleton, M.F., and Schmidt, P.W., 1982. Paleothermometry of the Sydney Basin: *Journal of Geophysical Research*, v. 87, p. 5351–5359.

Morley, M.E., Gleadow, A.J.W., and Lovering, J.F., 1981. Evolution of the Tasman Rift: Apatite fission track dating evidence from the southeastern Australian continental margin, *in* Cresswell, M.M., and Vella, P., eds., *Gondwana Five*: Rotterdam, A.A. Balkema, p. 289–293.

Ruxton, B.P., and McDougall, J., 1967. Denudation rates in northeast Papua from potassium-argon dating of lavas: *American Journal of Science*, v. 265, p. 545–561.

Stephenson, R.S., and Lambeck, K., 1985. Erosion-isostatic rebound models for uplift: An application to south-eastern Australia: *Geophysical Royal Astronomical Society Geophysical Journal* (in press).

Taylor, G., 1978. A brief Cainozoic history of the upper Darling basin: *Royal Society of Victoria Proceedings*, v. 90, p. 53–59.

Veevers, J.J., 1982. Australian-Antarctic depression from the mid-ocean ridge to adjacent continents: *Nature*, v. 295, p. 315–317.

Wass, S.Y., and Hollis, J.D., 1983. Crustal growth in south-eastern Australia—Evidence from lower crustal eclogitic and granulitic xenoliths: *Journal of Metamorphic Petrology*, v. 1, p. 25–45.

Wellman, P., 1979. On the Cainozoic uplift of the southeastern Australian highland: *Geological Society of Australia Journal*, v. 26, p. 1–9.

Wellman, P., and McDougall, I., 1974. Potassium-argon ages on the Cainozoic volcanic rocks of New South Wales: *Geological Society of Australia Journal*, v. 21, p. 247–272.

Woolley, D.R., 1978. Cainozoic sedimentation in the Murray drainage basin, New South Wales section: *Royal Society of Victoria Proceedings*, v. 90, p. 61–65.

Young, R.W., 1983. The tempo of geomorphological change: Evidence from southeastern Australia: *Journal of Geology*, v. 91, p. 221–230.

Young, R.W., and Bishop, P., 1980. Potassium-argon ages on Cainozoic volcanic rocks in the Crookwell-Goulburn area, New South Wales: *Search*, v. 11, p. 340–341.

ACKNOWLEDGMENTS

I thank Martin Williams and Gil Jones for their supervision of my thesis and for useful comments on this paper. I also thank Jim Bowler and Helene Martin for very helpful comments.

Manuscript received October 17, 1984
 Revised manuscript received April 1, 1985
 Manuscript accepted April 18, 1985

Figure 1. Maps showing the location of the Española basin and the area of this report (after Manley, 1979). a. Map of basins along the Rio Grande in northern New Mexico and southern Colorado (stippled areas), and surrounding mountains.

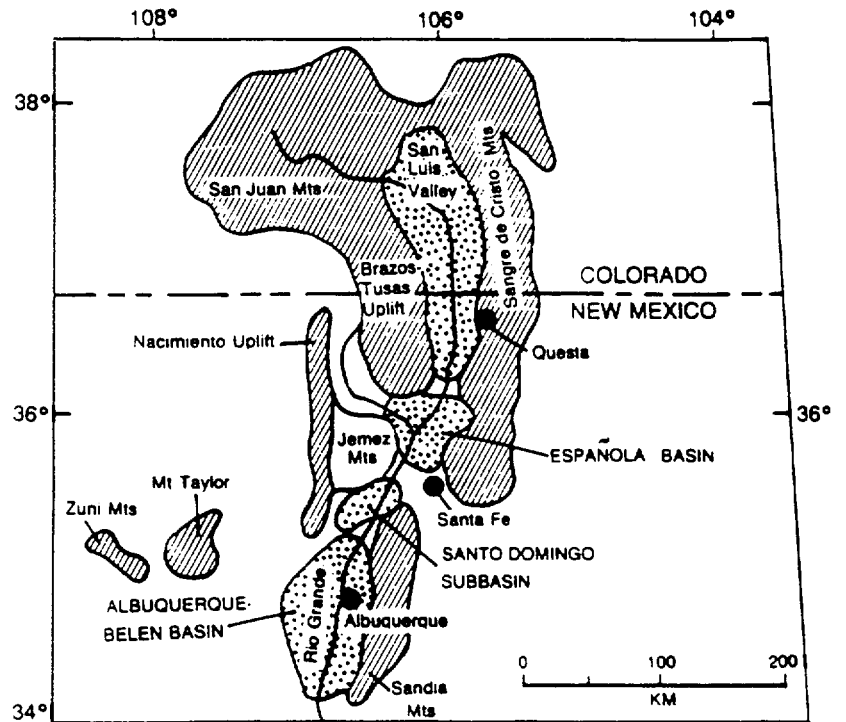
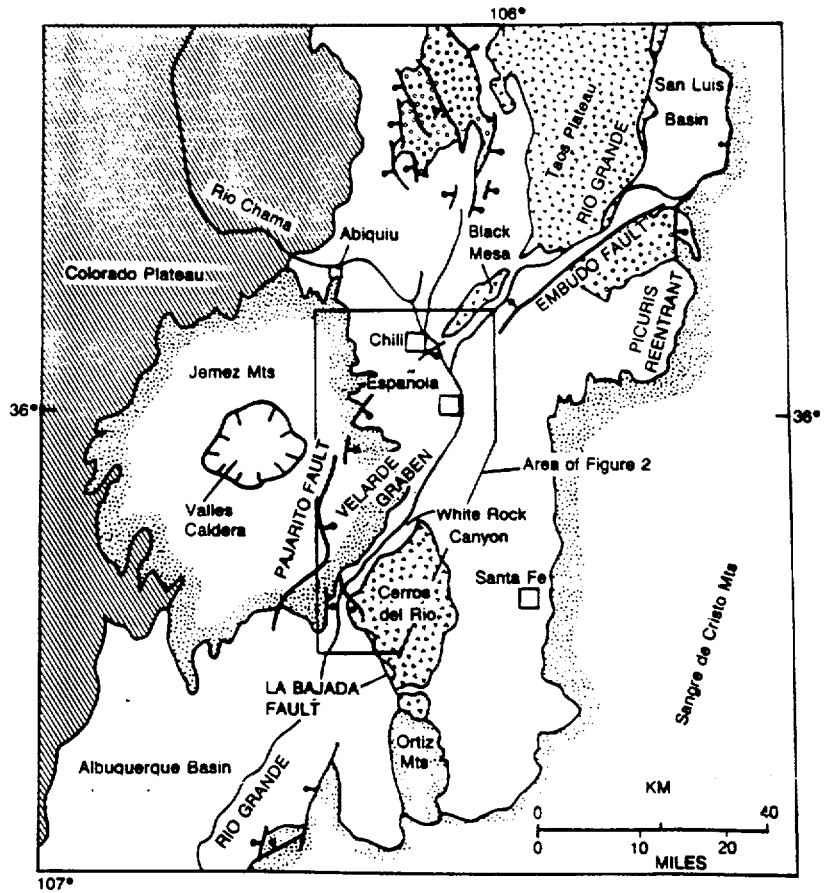


Figure 1. (Continued). b. Generalized geology of the Española basin, which extends from the La Bajada fault to the southeast edge of the Taos Plateau. Basin is bounded by Precambrian and lower Paleozoic rocks of the Sangre de Cristo Mountains, Mesozoic rocks of the Colorado Plateau, and Tertiary and Quaternary volcanic rocks of the Jemez Mountains. Principal rock types exposed in the basin are Precambrian metamorphic and igneous rocks (circle pattern), upper Tertiary sedimentary rocks (unpatterned), and upper Miocene and Pliocene basaltic rocks (angle pattern).



**CLIMATE-CHANGE INDUCED SEDIMENT-YIELD
VARIATIONS FROM ARID AND HUMID HILLSLOPES --
IMPLICATIONS FOR EPISODES OF QUATERNARY AGGRADATION**

No 100054

BULL, William B., Geosciences Dept., Univ. Arizona, Tucson, AZ, 85721

Quaternary climatic changes may have been synchronous in the fluvial systems of Southern California, but the timing of aggradation episodes may vary between drainage basins. Spatial variations of times of maximum aggradation result from 1) different response times of fluvial processes to climatic perturbations in watersheds of different size, slope, and lithology, 2) altitudinal variations in climate-controlled sediment-yield processes, and 3) effects of concurrent uplift on sediment yield and stream power.

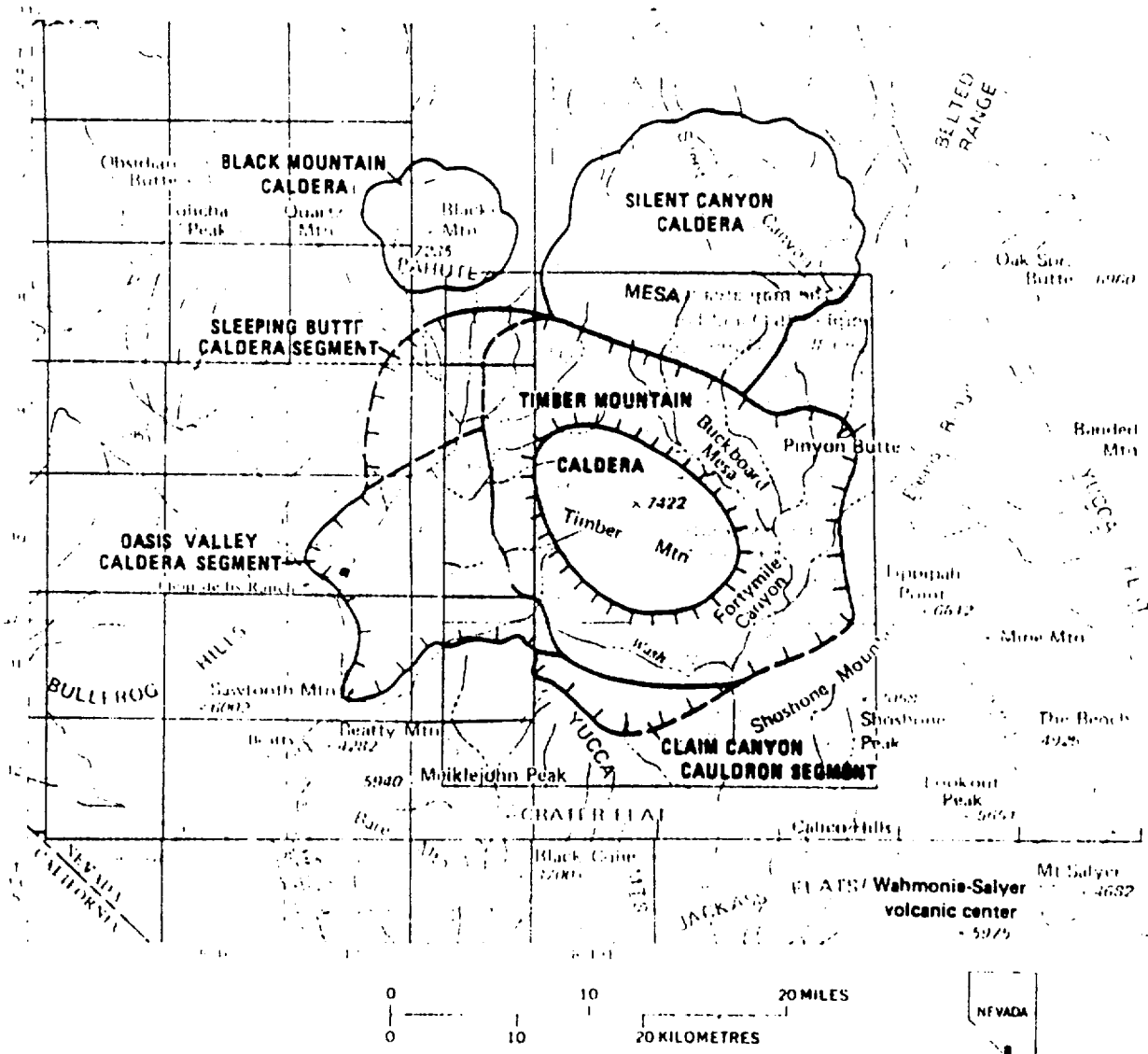
Process-response models of the impact of Pleistocene-Holocene climatic changes on simple watersheds in California and New Zealand illustrate the potential for complications in the large-altitude-range drainage basins of the Transverse Ranges. Monolithologic hillslopes in strongly seasonal, arid, hyperthermic, tectonically inactive drainage basins of the Mojave Desert accumulated colluvium during full-glacial climates, which was stripped during the early Holocene to aggrade valleys. Monolithologic hillslopes in the weakly seasonal, humid, mesic to frigid Charwell River basin of New Zealand had maximum sediment yields in a periglacial environment during full-glacial climates; sediment yield decreased during the Holocene and streams degraded valley fills. Thus hillslopes in different climatic regimes may have undergone markedly different vegetation, sediment-yield, and water-yield changes during the latest Pleistocene and early Holocene, resulting in either aggradation or degradation of the stream subsystem.

Spatial variation of factors influencing hillslope sediment-yield rates and stream power in the Transverse Ranges may result in drainage-basin aggradation events at similar or at dissimilar times. Each fluvial system has responded differently to the Pleistocene-Holocene climatic change. Within complex basins, different process-response models should be used for high slopes subject to Pleistocene periglacial processes than for low semiarid slopes subject to fluvial processes.

HQS. 880517.1107

GEOLOGIC MAP OF THE TIMBER MOUNTAIN CALDERA AREA,
 NYE COUNTY, NEVADA

By F. M. Byers, Jr., W. J. Carr, Robert L. Christiansen,
 P. W. Lipman, Paul P. Orkild, and W. D. Quinlivan



EXPLANATION

- Approximate outer limit of Timber Mountain-Oasis Valley caldera complex. Includes Sleeping Butte and Claim Canyon segments. Dashed where indefinite
- Periphery of Timber Mountain resurgent dome
- Timber Mountain caldera area map

FIGURE 1. -- Southwestern Nevada volcanic field showing relation of Timber Mountain caldera area to major volcanic centers

INTRODUCTION

The southwestern Nevada volcanic field (fig. 1) is a faulted, dissected volcanic plateau composed of silicic ash-flow tuffs and subordinate lavas, ranging in age from mid-Miocene to mid-Pliocene, or about 16 to 6 m.y. (million years) old (Kistler, 1968; Marvin and others, 1970, p. 2669). It includes mainly the Timber Mountain-Oasis Valley caldera complex flanked by the peralkaline Silent Canyon and Black Mountain calderas on the north. The volcanic activity reached a maximum between about 14 and 11 million years ago, when cauldron subsidences accompanied by eruption of voluminous ash flows occurred at the Sleeping Butte, Silent Canyon, Claim Canyon, Timber Mountain, and possibly Oasis Valley centers (fig. 1).

The nine 7½-minute quadrangles included in the Timber Mountain caldera area were mapped mainly between 1960 and 1965 by the authors and by R. E. Anderson, H. R. Cornwall, David Cummings, E. N. Hinrichs, F. J. Kleinhampl, R. D. Krushensky, S. J. Luft, D. C. Noble, J. T. O'Connor, and C. L. Rogers. (See index on map sheet.) Eight of the quadrangles were mapped and published at a scale of 1:24,000. Bare Mountain NE quadrangle in the southwestern corner of the map area was mapped by Cornwall and Kleinhampl (1961) and later by Paul P. Orkild, P. W. Lipman, and W. D. Quinlivan. Quadrangles mapped by the U.S. Geological Survey of the Southwestern Nevada volcanic field and the Nevada Test Site are shown on the index. (See also references at end of "Description of map units.")

The authors have generalized and revised previous mapping using additional field, petrographic, isotopic-age, and magnetic-polarity data, resulting in simplification of the stratigraphy and clarification of the geologic structure. For example, the thick ash-flow tuff exposed on Timber Mountain resurgent dome (fig. 1), originally mapped as tuff of Cat Canyon, is now known to be the intracaldera accumulation of the Ammonia Tanks Member of the Timber Mountain Tuff. Stratigraphic revisions implemented on the accompanying map explanation are discussed in U.S. Geological Survey Professional Paper 919 (Byers and others, 1975).

TERMINOLOGY

The terminology of tuffs is adapted from Smith (1960) and Ross and Smith (1961). As used here, "tuff" without a modifier means ash-flow tuff. Other kinds of tuff are indicated by appropriate modifiers. Volcanic names are based on chemical analyses or on phenocryst compositions (Rittmann, 1952, p. 77) where chemical analyses are not available. The use of "quartz latite" is a convenient term for mafic crystal-rich tuffs containing 65-72 percent silica, in contrast to mafic-poor, more silicic tuffs. The term "high-silica rhyolite" designates tuffs in the 76-78 percent range of silica.

The terms "caldera" and "cauldron" refer respectively to a large topographic depression of volcanic origin and the corresponding subsided structural block. The term "caldera" includes filled and buried calderas. This extension of the definition of Williams (1941, p. 242) to include buried cal-

deras is in keeping, for example, with his usage of the term "Medicine Lake caldera of northern California" (Williams, 1941, p. 296; Anderson, 1941, p. 358). The Claim Canyon cauldron segment (fig. 1) is not a depression but a topographically high block of thick intracaldera tuffs that have been eroded into mountainous topography, similar to the classic Glen Coe cauldron of Scotland (Clough and others, 1909; Williams, 1941, p. 296). The term "segment" is applied to a part of a caldera or cauldron that is truncated by a later subsidence.

In figure 1 and on the geologic map the caldera boundaries shown are the approximate main structural limits of the collapsed area, based on geologic and geophysical information. Locally, caldera boundaries determined by erosion are shown where geophysical and structural evidence is lacking. Potassium-argon ages, in millions of years (Kistler, 1968; Marvin and others, 1970), and sign of magnetic polarity (G. D. Bath, oral and written commun., 1971), where known, are included in the "Description of Map Units" that follows.

DESCRIPTION OF MAP UNITS

Qac	ALLUVIUM AND COLLUVIUM (QUATERNARY) - Unconsolidated bouldery to sandy stream deposits, alluvial fans, talus, and slope-wash deposits. 0-60+ m (0-200+ ft)
QTb	TRACHYBASALT LAVAS (QUATERNARY OR TERTIARY) - Grayish-black massive to vesicular olivine-bearing trachybasalt and cinders. Thickness 0-76 m (0-250 ft)
	THIRSTY CANYON TUFF (PLIOCENE)
Ttg	Gold Flat Member - Simple ash-flow tuff cooling unit, yellowish- to reddish-brown, pantelleritic composition, partly to densely welded. Thickness 0-30± m (0-100± ft)
Ttt	Trail Ridge Member - Simple ash-flow tuff cooling unit, purplish-brown in densely welded upper part to pale-pink in nonwelded lower part; comenditic rhyolite composition. Included with unit are 0-3 m (0-10 ft) of white to buff pumiceous ash-fall tuff under the ash-flow tuff. Phenocrysts (1-4 mm), 2-30 percent, mainly sanidine with less abundant iron-rich clinopyroxene, fayalitic olivine, opaque oxides, and accessory biotite, zircon, and apatite. Mapped with Spearhead and Rocket Wash Members in cross sections and locally under Buckboard Mesa. Thickness 0-60± m (0-200± ft)
Tts	Spearhead and Rocket Wash Members - Two compound ash-flow tuff cooling units, yellowish-gray to dark-reddish-brown, with thin buff pumice lapilli ash-fall tuff at base of each unit. Composition trachytic soda rhyolite to comendite. Spearhead Member, 0-60± m (0-200± ft) thick, nonwelded to densely welded; Rocket Wash Member, 0-120+ m (0-400+ ft) thick, nonwelded to partly welded. Phenocrysts 3-25 percent (1-5 mm), mainly sodic sanidine in Spearhead Member

	and mainly sanidine-anorthoclase and sodic plagioclase in Rocket Wash Member, with sparse quartz, iron-rich clinopyroxene, and fayalitic olivine, amphibole, opaque oxides, biotite, apatite, and zircon. Some ash flows contain abundant dark-gray scoriaceous pumice lenses as much as 60 cm (2 ft) in diameter. K-Ar age 7.5 m.y. (million years)		ash-fall pumice-lapilli tuff beds genetically related to Shoshone Mountain rhyolite center, and a few vitric shard tuff beds less than 60 cm (2 ft) thick. In western part of mapped area, unit intertongues with tuff beds mapped as ash-fall and nonwelded tuff (Tan). Thickness 0-300 ± m (0-1,000 ± ft)
Tlp	LAVAS OF PILLAR SPRING (PLIOCENE) Medium- to brownish-gray trachytic lava flows, dense to vesicular, containing 25-40 percent phenocrysts (1-5 mm) of sodic plagioclase and anorthoclase, and sparse clinopyroxene, olivine, opaque oxides, apatite, and zircon. Thickness 0-300+ m (0-1,000+ ft)	Tan	Ash-fall and nonwelded tuff -- Light-colored zeolitized bedded tuff (largely ash falls of diverse provenance) and local nonwelded ash-flow tuffs that accumulated mainly within Timber Mountain caldera. Intertongues with gravel and tuffaceous sediments (Tgs), and rhyolite lavas in Timber Mountain caldera (Trf, Trbw, Trcc). Thickness 0-600+ m (0-2,000+ ft)
Tlr	LAVAS OF RIBBON CLIFF (PLIOCENE) - Medium- to brownish-gray massive to flow-layered dense to vesicular trachytic soda rhyolite, quartz trachyte, and trachyte lavas; contains 15-30 percent phenocrysts, mainly large (as much as 2 cm) anorthoclase with sparse clinopyroxene. Relation to rhyolite lavas of Shoshone Mountain (Trs, Trsi) and mafic lavas (Tlf) uncertain; locally overlies mafic lavas. Thickness 0-700+ m (0-700+ ft)	Tdf	Debris flows and breccia -- Thick-bedded debris flows with pale-orange tuffaceous matrix, grading downward into megabreccia consisting of very poorly sorted angular fragments as much as 6 m (20 ft) in diameter with little or no fine tuff matrix. At test well 8 in Falcon Canyon, tuffaceous debris beds are separated from underlying megabreccia by the upper quartz-latitude subunit of the Rainier Mesa Member (Tmr) of the Timber Mountain Tuff. In drill hole UE18r and in surface exposures inside caldera wall, breccia contains blocks of densely welded Rainier Mesa Member, of Tiva Canyon (Tpc) and Topopah Spring (Tpt) Members of the Paintbrush Tuff, and of rhyolite lavas associated with Claim Canyon caudron. Thickness 0-300+ m (0-1,000+ ft)
Trs	RHYOLITE LAVAS OF SHOSHONE MOUNTAIN (PLIOCENE) -- Four similar lava flows, increasing in volume downward; each flow includes devitrified light-brownish-gray to grayish-orange-pink finely flow banded rhyolite grading downward to vitric tuff-breccia in lower few tens of feet. Sparse alkali feldspar phenocrysts. Thickness 0-300 ± m (0-1,000 ± ft)	Trf	RHYOLITE LAVAS OF FORTY MILE CANYON (PLIOCENE) -- Gray and pastel-colored devitrified rhyolite, locally vitrophyric in lower part. Includes ash-fall tuff, locally fused tuff (Christiansen and Lipman, 1966), and breccia rubble between flows. Youngest lava overlies middle part of mafic lavas (Tlf); locally includes rhyolite lavas of Beatty Wash (Trbw) at base. Thickness 0-330 ± m (0-1,100 ± ft)
Trsi	Intrusive rhyolite -- Massive light-gray strongly devitrified nearly aphyric rhyolite of composition similar to rhyolite lavas of Shoshone Mountain. Thickness 0-300 ± m (0-1,000 ± ft)	Trfd	Feeder dike -- Coarse unsorted tuff breccia and gray devitrified to vitrophyric rhyolite; flow-banded rhyolite is partly brecciated and included in tuff breccia, and in places intrudes tuff breccia
Tlf	MAFIC LAVAS (PLIOCENE) -- Dark-gray porphyritic lavas and minor intercalated scoriaceous rubble and cinder beds; dense to vesicular. At Dome Mountain, upper and middle flows are trachyandesite; lower flows, basalt; mineralogy given in Luft (1964, p. D16); the upper and middle lavas of trachyandesite are distinguished from the lower basaltic lavas by common resorbed plagioclase phenocrysts as much as 1 cm in length. Thickness 0-300 ± m (0-1,000 ± ft)	Tcr	TUFF OF CUTOFF ROAD (PLIOCENE) -- Simple ash-flow cooling unit. Moderately welded light-gray to tan microcrystalline upper part grades down to nonwelded pinkish-gray nearly glassy lower part. Nonwelded and locally sericitized in southwestern Timber Mountain caldera moat area; zeolitized, white to very light gray, pastel-weathering, on northeast flank of resurgent dome. Petrographically like rhyolite lavas of Beatty Wash (Trbw). Thickness 0-120 ± m (0-400 ± ft). K-Ar age 9.5 m.y.; magnetic polarity, reversed
	SEDIMENTARY ROCKS AND DEBRIS MOSTLY WITHIN TIMBER MOUNTAIN CALDERA - (PLIOCENE)	Trbw	RHYOLITE LAVAS OF BEATTY WASH (PLIOCENE) -- Lava flows, vitrophyric in upper and
Tgs	Gravel and tuffaceous sediments -- Upper part is caliche-cemented fan gravel with blocks as much as 3 m (10 ft) in diameter grading downward into finer, rounded friable cobble conglomerate. Lower part includes gravel intertonguing with tuffaceous friable sandstone, a few light-gray		

- lower parts, lithologically like rhyolite lavas of Fortymile Canyon (Trf); plagioclase locally altered to sericite in southern moat area. Correlated with petrographically similar tuff of Cutoff Road (Tcr). Thickness 0-300± m (0-1,000± ft). Magnetic polarity, reversed
- Ttf TUFFS OF FLEUR-DE-LIS RANCH (PLIOCENE)** - Simple cooling unit, light-purplish-brown to yellowish-gray, with common small (0.5-1.0 mm) biotite flakes. Intruded and overlain by rhyolite lava of West Cat Canyon (Trcc) at volcanic vent south of Beatty Wash. Probably thickens downward as inferred in Timber Mountain caldera moat (section B-B'). Near the Fleur-de-lis Ranch (fig. 1), consists of three moderately to densely welded cooling units with one intercalated lava flow that is petrographically similar to rhyolite lava of West Cat Canyon (Trcc). Thickness 0-152± m (0-500± ft). Magnetic polarity of uppermost tuff, normal
- Trcc RHYOLITE LAVAS OF WEST CAT CANYON (PLIOCENE)** - Dark- and light-gray glassy or light-yellowish-brown to pale-red devitrified rhyolite lava with common tiny (< 1.5 mm) plagioclase and biotite phenocrysts. Intrude, intertongue with, locally overlie, and are petrographically similar to tuffs of Fleur-de-lis Ranch. Thickness 0-300± m (0-1,000± ft)
- Trm RHYODACITIC AND MAFIC LAVAS (PLIOCENE)** - Light-gray to gray to purplish-gray thick rhyodacite lava flow on east side of Timber Mountain; elsewhere, scattered exposures of trachyandesite and basalt(?), locally scoriaceous and palagonitized, are included. Mafic lavas contain calcic plagioclase, clinopyroxene, and sparse orthopyroxene and olivine phenocrysts. Rhyodacite lava flow contains conspicuous andesine phenocrysts as much as 5 mm in length. Thickness 0-150± m (0-500± ft). Relation to tuffs of Cutoff Road (Tcr) and Fleur-de-lis Ranch (Ttf) and to rhyolite lavas of Beatty Wash (Trbw) and West Cat Canyon (Trcc) is uncertain
- INTRUSIVE ROCKS ON TIMBER MOUNTAIN (PLIOCENE)**
- Ttd Tuff dike zone** - Zone as much as 152 m (500 ft) wide, composed of possible cone sheets individually ranging from 2.5 cm (1 in.) to 9 m (30 ft) in width, intrusive into lower quartz-latite subunit of Ammonia Tanks Member (Tml) of Timber Mountain Tuff; roughly concentric with Timber Mountain resurgent dome on east flank. Individual dikes are high-silica rhyolite, very light gray, and devitrified and contain light-brown xenoliths of lower part of Ammonia Tanks Member. Pumice lenticles are flattened, but no flow laminations are present.
- Tg Microgranite porphyry** - Light-gray; feldspar phenocrysts as large as 9 mm in a fine-grained (0.2-0.5 mm) groundmass; many feldspar phenocrysts consist of thick alkali feldspar jackets mantling small cores of oligoclase; groundmass consists of alkali feldspar (75-85 percent), quartz (10-20 percent), plagioclase (0-10 percent), and rare to sparse apatite, zircon, and allanite
- Tri Intrusive rhyolite** - Rhyolite dikes and small plugs, purplish-gray, dense; flow-layered dikes highly brecciated, probably autoclastic. High-silica rhyolite plugs in East Cat Canyon are stony, light gray to white, flow layered, and mineralogically similar to high-silica rhyolite of Ammonia Tanks Member (Tmu) of Timber Mountain Tuff. Rhyolite plug at Parachute Canyon is light gray, glassy to stony, porphyritic, flow layered, locally lithophysal; basal vitrophyre at northwest edge of plug
- TIMBER MOUNTAIN TUFF (PLIOCENE)** - Five closely related and petrographically similar ash-flow cooling units characterized by quartz phenocrysts. The Rainier Mesa and Ammonia Tanks Members are voluminous compositionally zoned compound cooling units, probably composite sheets, each exceeding 1,000 km³ (250 mi³) in volume. The overlying three tuffs have a combined volume of less than 200 km³ (50 mi³) and are confined to Timber Mountain and Oasis Valley calderas; uppermost two tuffs mapped as one unit - tuffs of Crooked Canyon. Size of phenocrysts larger (as much as 3 mm) in the Rainier Mesa and Ammonia Tanks Members than in overlying units. The Ammonia Tanks Member here includes the tuff of Cat Canyon and tuff of Camp Transvaal of earlier reports (Carr and Quinlivan, 1966; Lipman, Quinlivan, Carr, and Anderson, 1966)
- Tmc Tuffs of Crooked Canyon** - Two similar simple cooling units of homogeneous nonwelded to partly welded rhyolite. Upper tuff is gray to pale orange; lower tuff, commonly pale pinkish purple. Upper tuff is slightly more mafic than lower tuff. On east flank of Timber Mountain near tuff dike zone (Ttd) both units contain common light-brown xenoliths of lower quartz-latite subunit of Ammonia Tanks

- Member (Tml). Thickness 0-300± m (0-1,000± ft)
- Tmb** Tuff of Buttonhook Wash -- Compound cooling unit consisting of an upper, reddish- to purplish-brown densely welded quartz latite and a lower, light-gray nonwelded to partly welded high-silica rhyolite. Contains sparse small mafic lithic and purplish-brown quartz latitic inclusions of Ammonia Tanks (Tmu, Tml) and Rainier Mesa (Tmr) Members. Separated from the underlying Ammonia Tanks Member by a few inches to a few feet of shard-rich bedded tuff. Thickness 0-250± m (0-800± ft)
- Tmu** *Upper part* - On Timber Mountain resurgent dome multiple ash-flows consist of several light-purplish-gray nonwelded to moderately welded rhyolitic zones grading up into and alternating with brown densely welded quartz latite zones. This sequence thins eastward and is overlain on the east side of Timber Mountain by nonwelded porous high-silica rhyolite tuff, which contains common light-brown quartz latite xenoliths of lower part of Ammonia Tanks Member (Tml). Away from Timber Mountain dome, upper part (Tmu) is light-brownish-gray nonwelded to black densely welded glassy quartz latite tuff, less than 90 m (300 ft) thick, underlain by local thin pink to light-gray high-silica rhyolite in northern part of mapped area; this local rhyolite is probably equivalent to rhyolite of lower part of Ammonia Tanks (Tml) elsewhere. Quartz latite is characterized by large dark-gray to black scoriaceous lenticles as much as 61 cm (2 ft) in length and purplish-gray rounded xenoliths of Rainier Mesa Member as much as 30 cm (1 ft) in diameter. Thickness 0-250± m (0-800± ft). K-Ar age, 11.1 m.y.; magnetic polarity, normal
- Tml** *Lower part* -- On Timber Mountain Dome, multiple ash flows consist of brown, purplish-gray, and light-gray dense crystalline locally granophyric moderately welded quartz latite tuff intertonguing with nonwelded to partly welded less mafic tuff in lower part overlain by rhyolite of variable phenocryst composition. Locally in southeastern part of mapped area, an uppermost thin quartz latite that is probably the quartz latite caprock of the upper part of the Ammonia Tanks (Tmu) is included in the lower part. Largely equivalent to tuff of Camp Transvaal of an earlier report (Lipman, Quinlivan, Carr, and Anderson, 1966). Thickness 0-600+ m (0-2,000+ ft). K-Ar age, 11.1 m.y.; magnetic polarity, normal
- Tmr** Rainier Mesa Member -- Compositionally zoned compound-cooling unit. Near Timber Mountain caldera commonly has brown to gray rubbly quartz latite caprock characterized by a vapor-phase zone, a middle purple aphanitic densely welded locally glassy high-silica rhyolite, and a lower conspicuously pink glassy nonwelded high-silica rhyolite. In other areas a dark glassy densely welded quartz latite caprock overlies a vapor-phase zone of the middle rhyolite. Inside Timber Mountain caldera, the quartz latite caprock subunit is intercalated with the debris flows and breccia (Tdf) in Beatty Wash and Falcon Canyon, where it contains xenoliths of caldera-wall rocks and sparse granitic rocks. Thickness 0-600+ m (0-2,000+ ft). K-Ar age, 11.3 m.y.; magnetic polarity, reversed
- Trma** PRE-AMMONIA TANKS RHYOLITE LAVAS (PLIOCENE) -- Lavas confined to Timber Mountain caldera. Light-gray glassy porous breccia in uppermost zones; pale red flow laminated to light gray massive microcrystalline in middle of flow, dark glassy in lower zones. Composition is high-silica rhyolite like that of similar facies in the upper part of Ammonia Tanks Member (Tmu) of the Timber Mountain Tuff. Rhyolite lava penetrated beneath Ammonia Tanks Member (Tmu, Tml) in drill hole UE18r at 1,099-m (3,605-ft) depth is similar but has fewer phenocrysts. Thickness 0-250± m (0-800± ft). Magnetic polarity, reversed
- Trmr** PRE-RAINIER MESA RHYOLITE LAVAS (PLIOCENE) -- Upper zones are porous glassy breccia; middle zones, pale red and reddish purple, microcrystalline; lower zones, dark gray, glassy. Two petrographic types of quartz-rich lavas: one, probably the younger, is high-silica rhyolite, petrographically very similar to that of the Rainier Mesa Member; the other lava, probably older, is transitional in phenocryst composition between the Paintbrush and the Timber Mountain Tuffs. This lava (Trmr) was penetrated under Pahute Mesa in drill holes U20a and U20a-2 north of the caldera and was called quartz-rich rhyolite lava of Scrugham Peak quadrangle (Byers and Cummings, 1967; Orkild, Sargent, and Snyder, 1969); south of the caldera, lavas nearly identical in composition to the north one were called rhyolite of Windy Wash (Christiansen and Lipman, 1965). Thickness 0-300± m (0-1,000± ft). K-Ar age of high-silica rhyolite, 11.3 m.y.
- Feeder dikes -- Coarse unsorted tuff breccia and light-gray devitrified to black glassy rhyolite; fluidal rhyolite intrudes tuff breccia but is also brecciated and included in tuff breccia
- PAINTBRUSH TUFF (MIOCENE) -- Quartz-free to quartz-poor sequence of five peraluminous rhyolitic to quartz latitic simple and compound ash-flow tuff cooling units, locally separated by bedded tuff, rhyolite lava flows near

- source area, and tuff breccia. Color generally indicative of cooling or crystallinity zones: dark gray to black, glassy; brownish gray, cryptocrystalline; light brownish to purplish-gray, microcrystalline; and light gray to light purplish gray, coarsely microcrystalline with granophyric pumice. A granophyric facies occurs in middle parts of thickened members inside Claim Canyon cauldron segment
- Tp** Tuff of Pinyon Pass -- Simple cooling unit. Upper quartz-latic subunit is brown, purplish brown, pale orange, and light gray and moderately to densely welded and contains relict dark glassy crystal-rich pumice lenticles and minor white rhyolitic pumice lenticles 1-10 cm (½-4 in.) in length. The middle high-silica rhyolitic subunit is pale purplish gray, partly welded. The lower rhyolitic subunit is yellowish gray to reddish brown, is moderately to densely welded, contains minor crystal-rich quartz-latic pumice lenticles, and grades down to pinkish-gray nonwelded glassy to zeolitic. Unit similar to Tiva Canyon Member (Tpc). Thickness 0-150± m (0-500± ft)
- Tpm** Tiva Canyon Member -- Compositionally zoned compound cooling unit
- Tpm** Tuff of Chocolate Mountain - Thick accumulation of uppermost quartz-latic caprock facies confined within Claim Canyon cauldron. Three subunits can be distinguished where the tuff breccia (Tbx) intertongues with the tuff of Chocolate Mountain: upper subunit is densely welded and brown microcrystalline to black glassy; middle subunit is less glassy but otherwise similar to upper; lower subunit is the thickest, is densely welded, brown microcrystalline to light-gray granophyric, and contains xenoliths of Yucca Mountain Member (Tpy), Pah Canyon Member (Tpp), rhyolite lavas between Pah Canyon and Yucca Mountain Members (Trp), and Crater Flat Tuff (Tcf). Thickness 0-600± m (0-2,000± ft). K-Ar age, 12.6 m.y.; magnetic polarity, reversed
- Tpc** Main part -- Upper quartz-latic subunit is similar to upper subunit of tuff of Pinyon Pass (Tp). Middle rhyolitic subunit is moderately welded, purplish gray, and locally lithophysal; contains crystal-rich quartz-latic gray to dark-gray pumice lenticles that increase upward. Lower high-silica rhyolitic subunit is locally glassy and densely welded and grades down to dark-gray glassy to yellowish-gray zeolitized nonwelded shard-rich tuff; the lower subunit is distinguished from other Paintbrush subunits by hornblende, alkali feldspar, and sphene and a paucity of biotite. Thickness 0-900± m (0-3,000± ft). K-Ar age, 12.6 m.y.; magnetic polarity, reversed
- Tpy** Yucca Mountain Member -- Simple cooling unit, crystal poor. Brownish-gray to gray glassy nonwelded in uppermost and lowermost zones; middle zone is pale purplish gray to pale purplish brown, and shard rich and contains sparse small white pumice lenticles averaging about 1.3 cm (½ in.) in length and rare small grayish-red rhyolite xenoliths generally less than 1.3 cm (½ in.) in length. Where member exceeds 45 m (150 ft) in thickness, filled irregular light-colored lithophysal masses as much as 5 cm (2 in.) in diameter characterize middle zone. Thickness 0-300± m (0-1,000± ft)
- Tpp** Pah Canyon Member -- Yellowish- to light-brown moderately to densely welded simple cooling unit; contains abundant small pumice lenticles less than 1.3 cm (½ in.) in length and common small cognate xenoliths. Thickness 0-200± m (0-700± ft). Magnetic polarity, reversed
- Tpt** Topopah Spring Member -- Compound cooling unit. Upper part consists of 1.5-3 m (5-10 ft) of brownish-gray ash-fall pumice underlain by quartz latite ash-flow subunit, which contains abundant large dark-gray to black collapsed pumice lenticles as much as 30 cm (1 ft) in diameter. Middle part is black glassy to brown devitrified and contains abundant large cognate and accidental xenoliths, including granite. Lower part is rhyolite subunit consisting of mottled gray and brown devitrified rhyolite containing sparse crystal-rich pumice lenticles, underlain by crystal-poor black densely welded glassy to pinkish-brown nonwelded glassy ash-flow tuff subunit. Thickness 0-300± m (0-1,000± ft). K-Ar age, 13.2 m.y.; magnetic polarity, normal
- Trpc** POST-TIVA CANYON RHYOLITE LAVAS (MIOCENE) -- Two purplish-gray to light-gray rhyolite lava flows commonly separated by bedded tuff. Penetrated in drill holes U20a-2, and UE20c on Pahute Mesa. Upper and lower flow mapped as quartz-bearing rhyolite and biotite-bearing rhyolite, respectively, of rhyolite lavas of Scrugham Peak quadrangle (Byers and Cummings, 1967; Orkild and others, 1969). Both lavas have enclosing breccia and glassy zones with a central devitrified core. Thickness 0-350 m (0-1,140 ft). Magnetic polarity, reversed
- Trp** RHYOLITE LAVAS BETWEEN YUCCA MOUNTAIN AND PAH CANYON MEMBERS (MIOCENE) -- Zoned light-brownish-gray, light-purplish-gray, and light-gray lavas similar in outcrop appearance and hand specimen to post-Tiva Canyon rhyolite lavas (Trpc). Three lavas are exposed in north wall of Timber Mountain caldera: two are in sequence, hornblende-bearing rhyolite lavas of Scrugham Peak quadrangle and the underlying pyroxene-bearing rhyolite (Byers and Cummings, 1967;

- Orkild and others, 1969), characterized by high ratio of alkali feldspar to total feldspar like that of Tive Canyon Member (Tpc) of the Paintbrush Tuff; a local quartz- and hornblende-bearing lava is also included. The rhyolite lavas on the south side of Timber Mountain caldera are similar to the lower pyroxene-bearing lava on the north side. Thickness 0-360 ± m (0-1,200 ± ft)
- Trpp PRE-PAH CANYON RHYOLITE LAVAS (MIOCENE)** Two lava flows under Pah Canyon Member (Tpp) of Paintbrush Tuff, similar in appearance to lavas above (Trp) except for greater silicification but petrographically similar to one another and to the Pah Canyon. Faulted and fractured near boundary of Claim Canyon cauldron segment, where plagioclase and mafic minerals have been partly to completely destroyed by hydrothermal alteration. Thickness 0-180 ± m (0-600 ± ft). Magnetic polarity, reversed
- Tbx TUFF BRECCIA (MIOCENE)** - Light-yellowish-gray to grayish-yellow zeolitized massive poorly sorted tuff breccia with fine to coarse pumice matrix and many large blocks as much as several tens of feet across near wall of Claim Canyon cauldron segment, becoming less abundant and smaller away from wall. Blocks-to-matrix ratio as much as 4:1 near wall. Blocks consist largely of Pah Canyon (Tpp) and Yucca Mountain (Tpy) Members of Paintbrush Tuff, and subordinate rhyolite lavas between Pah Canyon and Yucca Mountain Members (Trp), and Crater Flat Tuff (Tcf); large blocks cracked. Thickness 0-150+ m (0-500+ ft)
- Tb BEDDED TUFF (MIOCENE)** - Light-colored locally zeolitized ash-fall tuff, thin-bedded to very thick bedded, locally massive; includes mostly ash-fall tuff of Paintbrush Tuff and tuffs and rhyolite lavas of Area 20; west of Split Ridge includes a local nonwelded ash flow named the tuff of Blacktop Buttes by Orkild and others (1969). Coarse-grained shard-crystal to lapilli-lithic tuff, the latter common near rhyolite vents, where unit includes minor fused tuff (Christiansen and Lipman, 1966) and welded ash fall. Includes thick ash falls genetically related to rhyolite lava extrusion and subordinate thin ash falls immediately underlying and locally overlying ash-flow tuffs. Locally includes reworked tuff and lenses of volcanic conglomerate. Phenocryst assemblage is quartz free to quartz poor in beds intercalated with members of Paintbrush Tuff; quartz-bearing, in beds intercalated with Stockade Wash Tuff and with tuffs and rhyolite lavas of Area 20. Thickness 0-360 ± m (0-1,200 ± ft)
- Tsw STOCKADE WASH TUFF (MIOCENE)** Simple cooling unit of ash-flow tuff, nonwelded to slightly welded, pale-gray to brown, containing abundant small orange pumice fragments less than 2.5 cm (1 in.) across. Phenocrysts less than 2.0 mm, including formerly euhedral quartz, moderately resorbed. Correlated with tuffs and rhyolite lavas of Area 20 (Tra) on the basis of petrographic similarity. Thickness 30-160 m (100-500 ft)
- Tra TUFFS AND RHYOLITE LAVAS OF AREA 20 (MIOCENE)** Zeolitized bedded and ash-flow tuffs and rhyolite lavas that fill Silent Canyon caldera (Orkild, Sargent, and Snyder, 1969). Phenocrysts, principally of quartz, feldspar, and biotite, range from a few percent to about 25 percent in the rhyolite lavas. With increase in phenocrysts, the feldspars in the lavas become larger, as much as 7 mm, and the plagioclase to total-feldspar ratio increases from a few percent to about 50 percent; broken resorbed quartz is typical of tuffs. The mafic and accessory minerals are biotite, allanite, and abundant hornblende in the lower lavas (K. A. Sargent, written commun., 1968). Thickness 0-1,500 ± m (0-5,000 ± ft)
- Tbg BELTED RANGE TUFF (MIOCENE)**
Grouse Canyon Member - Compound ash-flow cooling unit, comprising two distinct subunits of densely welded comenditic ash-flow tuff, greenish-gray to pale-brownish-gray and red, devitrified. Upper subunit contains 10-25 percent phenocrysts, largely sodic sanidine; lower subunit almost phenocryst-free at base, grading upward to about 5 percent phenocrysts at top. Lenticular granophyric pumice and gas cavities containing vapor-phase crystals of quartz, sanidine, and aegirine, with sodic amphibole common in upper subunit; conspicuously developed compaction and flow foliation and flow lineation, particularly in lower subunit. Sparse phenocrysts of sodic sanidine in lower subunit and very rare to sparse anhedral quartz, sodic amphibole, ferrosalite(?) (0.5-1.5 mm) aegirine-augite (0.2-0.5 mm) and fayalite; upper subunit has similar but more abundant phenocrysts without quartz. Thickness 0-75 m (0-250 ft). K-Ar age, 13.8 m.y. Magnetic polarity, normal
- Tbb Ash-fall tuff** - Gray glassy and yellow zeolitic fine to lapilli tuff; generally underlies the Grouse Canyon Member and is intercalated with flows of rhyolite lavas of Split Ridge (Trsr). Thickness 0-250 ± m (0-800 ± ft)
- Tbt Tub Spring Member** - Compound cooling unit of densely welded to nonwelded buff to bluish-gray and brick-red devitrified comenditic ash-flow tuff. Rock contains 20-25 percent phenocrysts of sodic sanidine (20-70

- percent), quartz (30-50 percent), and sparse aegirine-augite and fayalite; groundmass crystals include sparse acmite; lithic inclusions of rhyolite of Quartet Dome contain acmite and blue-green sodic amphibole in ground mass. Thickness 0-6+ m (0-20+ ft)
- Trsr **RHYOLITE LAVAS OF SPLIT RIDGE (MIOCENE)** - Flows and dikes, devitrified greenish-gray and brown nonporphyritic to very sparsely porphyritic, strongly flow-laminated; glassy basal zones and dike margins occur locally. Less than 1 percent phenocrysts of alkali feldspar, aegirine-augite, and fayalitic olivine. Intertongues with genetically related ash-fall tuff (Thb). Thickness 0-330+ m (0-1,100+ ft)
- Trq **RHYOLITE LAVAS OF QUARTET DOME (MIOCENE)** - Thick flows and endogenous domes of light-gray to grayish-red generally devitrified coarsely flow-layered comenditic lava; 5-30 percent phenocrysts of quartz, alkali feldspar, and sparse clinopyroxene and fayalite; groundmass contains acmite and blue-green sodic amphibole. Correlated with Tub Spring Member (Tbt) on basis of petrographic similarity. Thickness 0-300+ m (0-1,000+ ft)
- Tht **BIOTITE-HORNBLLENDE RHYOLITE WEST OF SPLIT RIDGE (MIOCENE)**
Ash-fall and nonwelded tuff - Pale-gray and yellow bedded and nonwelded zeolitized quartz-latic tuff containing locally common sub-angular to rounded fragments (1-10 cm) of dark welded tuff, mafic lava, and silicic lava; two thickest ash-flow tuffs (15 and 23 m; 50 and 75 ft) contain about 20 percent phenocrysts consisting mainly of predominant plagioclase and very minor alkali feldspar and quartz, and about 5 percent each of biotite and hornblende. Thickness 0-205 m (0-675 ft)
- Thl **Lava flows** - Two dark-bluish-gray glassy and orange to reddish-brown microcrystalline massive quartz latite flows. Upper flow contains about 10 percent phenocrysts consisting mainly of plagioclase, minor alkali feldspar and quartz, and about 10 percent dark minerals, including subequal biotite and hornblende; lower flow contains about 15 percent phenocrysts (as much as 5 mm), predominantly plagioclase, and about 15 percent dark minerals, biotite dominant over hornblende and magnetite. Accessory minerals in both flows include sphene, apatite, zircon, and allanite (K. A. Sargent, written commun., 1968). Thickness 0-250 m (0-820 ft). Magnetic polarity, reversed
- RHYOLITE LAVAS AND ZEOLITIZED TUFF (MIOCENE)** - Intertonguing or uncertain relations with Spring Member (Tbt), rhyolite lavas of Quartet Dome (Trq), biotite-hornblende rhyolite west of Split Ridge (Tht, Thl), and Crater Flat Tuff (Tcf)
- Trc **Rhyolite lavas of Calico Hills** - Light-gray, pale-purple, and pink devitrified microbrecciated and silicified lavas; glassy facies is light to dark gray or grayish green. Phenocrysts of quartz, alkali feldspar, plagioclase, and sparse magnetite and biotite. Overlies Crater Flat Tuff (Tcf). Thickness 0-460± m (0-1,500± ft)
- Tab **Zeolitized ash-flow and bedded tuff** - Massive and bedded porous white and pastel-colored pumiceous partially to completely zeolitized tuff. Beds are well sorted and locally cross stratified. Only uppermost part exposed along eastern border of mapped area; continuous with and equivalent to tunnel-bed sequence in Rainier Mesa quadrangle (Gibbons and others, 1963). Thickness 0-600± m (0-2,000± ft)
- Tcf **CRATER FLAT TUFF AND INTERCALATED LAVA FLOW (MIOCENE)** - In southern part of mapped area, the Prow Pass Member, the upper member, is similar but thinner (0-30± m), and separated from the Bullfrog Member, the lower member, by as much as 8 m (25 ft) of bedded tuff and breccia. The members are separated locally by an intercalated rhyolite lava flow that is not part of the Crater Flat Tuff. Over most of mapped area, Bullfrog Member is a nonwelded to densely welded, compositionally zoned ash-flow tuff cooling unit. In the northern part of the area the Prow Pass Member is missing. Both tuff members are brownish to purplish gray to light gray and contain phenocryst-poor small pumice lenticles averaging about 2.5 cm (1 in.) in length; absence of clinopyroxene distinguishes the Crater Flat Tuff from younger tuffs. Orthopyroxene and strongly resorbed quartz is diagnostic of the Prow Pass Member; Bullfrog Member contains hornblende and abundant biotite phenocrysts without orthopyroxene and is compositionally zoned with more mafic quartz-latic subunit in lower part; also characterized by an abundance of fine biotite (< 1 mm) in white pumice lenticles. In south wall of Oasis Valley caldera segment, Crater Flat Tuff is mapped with local intercalated lava flow similar mineralogically to underlying Bullfrog Member. Thickness 0-250± m (0-800± ft). K-Ar age of Bullfrog Member, 14.0 m.y. Magnetic polarity, normal
- Trv **REDROCK VALLEY TUFF (MIOCENE)** - Simple ash-flow cooling unit, greenish-gray, brick-red, brown, locally glassy. Resembles Crater Flat Tuff but has significantly less quartz. Penetrated in test well 8 (section C-C') and other drill holes east of mapped area. Alkali feldspar-total feldspar ratio

generally increases upward in unit; quartz also increases upward. Hornblende and biotite phenocrysts as much as 2.0 mm; quartz phenocrysts, small euhedra, length parallel to C axis less than 1 mm. Thickness 0-300 ± m (0-1,000 ± ft). K-Ar age, 15.7 m.y. Magnetic polarity, reversed

- Tvc TUFF AND CLASTIC ROCKS (MIOCENE?)
In sections only. Includes Fraction Tuff and possibly other ash-flow tuffs originating north of Timber Mountain area (Rogers and others, 1967) and minor bedded tuff and local fine and coarse clastic rocks generally at base of Tertiary sequence. Thickness 0-600 ± m (0-2,000 ± ft)
- Mej ELEANA FORMATION, UNIT J(?) (MISSISSIPPIAN) -- Light- to dark-gray silty laminated argillite, medium- to dark-gray and brown impure limestone containing thin (7.5-10 cm, 3-4 in.) sandy and silty interbeds, and conglomerate composed of rounded black chert, red argillite, and gray limestone; very thin bedded and brecciated. Thickness 0-30+ m (0-100+ ft)
- Did LIMESTONE AND DOLOMITE (DEVONIAN) -- Includes Devils Gate Lim. stone and Nevada Formation. Dark- to light-gray fine- to coarse-grained thin- to thick-bedded brecciated limestone and dolomite. Thickness 120 ± m (400 ± ft)

REFERENCES

- Anderson, C. A., 1941, Volcanoes of the Medicine Lake highland, California: California Univ. Dept. Geol. Sci. Bull., v. 25, p. 347-422.
- Barnes, Harley, Christiansen, R. L., and Byers, F. M., Jr., 1965, Geologic map of the Jangle Ridge quadrangle, Nye and Lincoln Counties, Nevada: U.S. Geol. Survey Geol. Quad. Map GQ-363.
- Barnes, Harley, Houser, F. N., and Poole, F. G., 1963, Geologic map of the Oak Spring quadrangle, Nye County, Nevada: U.S. Geol. Survey Geol. Quad. Map GQ-214.
- Burchfiel, B. C., 1966, Reconnaissance geologic map of the Lathrop Wells 15-minute quadrangle, Nye County, Nevada: U.S. Geol. Survey Misc. Geol. Inv. Map I-474.
- Byers, F. M., Jr., and Barnes, Harley, 1967, Geologic map of the Paiute Ridge quadrangle, Nye and Lincoln Counties, Nevada: U.S. Geol. Survey Geol. Quad. Map GQ-577.
- Byers, F. M., Jr., Carr, W. J., Orkild, P. P., Quinlivan, W. D., and Sargent, K. A., 1975, Volcanic suites and related cauldrons of Timber Mountain-Oasis Valley caldera complex, southwestern Nevada: U.S. Geol. Survey Prof. Paper 919. (In press.)
- Byers, F. M., Jr., and Cummings, David, 1967, Geologic map of the Scrugham Peak quadrangle, Nye County, Nevada: U.S. Geol. Survey Geol. Quad. Map GQ-695.
- Byers, F. M., Jr., Rogers, C. L., Carr, W. J., and Luft, S. J., 1966, Geologic map of the Buckboard Mesa quadrangle, Nye County, Nevada: U.S. Geol. Survey Geol. Quad. Map GQ-552.
- Carr, W. J., and Quinlivan, W. D., 1966, Geologic map of the Timber Mountain quadrangle, Nye County, Nevada: U.S. Geol. Survey Geol. Quad. Map GQ-503.
- Christiansen, R. L., and Lipman, P. W., 1965, Geologic map of the Topopah Spring NW quadrangle, Nye County, Nevada: U.S. Geol. Survey Geol. Quad. Map GQ-444.
- _____, 1966, Emplacement and thermal history of a rhyolite lava flow near Fortymile Canyon, southern Nevada: Geol. Soc. America Bull., v. 77, p. 671-684.
- Christiansen, R. L., and Noble, D. C., 1968, Geologic map of the Trail Ridge quadrangle, Nye County, Nevada: U.S. Geol. Survey Geol. Quad. Map GQ-774.
- Clough, C. T., Maufe, H. B., and Bailey, E. B., 1909, The cauldron-subsidence of Glen Coe; and the associated igneous phenomena: Geol. Soc. London Quart. Jour., v. 65, p. 611-678.
- Colton, R. B., and McKay, E. J., 1967, Geologic map of the Yucca Flat quadrangle, Nye County, Nevada: U.S. Geol. Survey Geol. Quad. Map GQ-582.
- Colton, R. B., and Noble, D. C., 1967, Geologic map of the Groom Mine SW quadrangle, Nye and Lincoln Counties, Nevada: U.S. Geol. Survey Geol. Quad. Map GQ-719.
- Cornwall, H. R., and Kleinhampl, F. J., 1961, Geology of the Bare Mountain quadrangle, Nevada: U.S. Geol. Survey Geol. Quad. Map GQ-157.
- _____, 1964, Geology of Bullfrog quadrangle and ore deposits related to Bullfrog Hills caldera, Nye County, Nevada, and Inyo County, California: U.S. Geol. Survey Prof. Paper 454-J, p. J1-J25.
- Ekren, E. B., Anderson, R. E., Orkild, P. P., and Hinrichs, E. N., 1966, Geology of Silent Butte quadrangle, Nye County, Nevada: U.S. Geol. Survey Geol. Quad. Map GQ-493.
- Ekren, E. B., Anderson, R. E., Rogers, C. L., and Noble, D. C., 1971, Geology of northern Nellis Air Force Bombing and Gunnery Range, Nye County, Nevada: U.S. Geol. Survey Prof. Paper 651, 91 p.
- Ekren, E. B., Rogers, C. L., Anderson, R. E., and Botinelly, Theodore, 1967, Geologic map of the Belted Peak quadrangle, Nye County, Nevada: U.S. Geol. Survey Geol. Quad. Map GQ-606.
- Ekren, E. B., and Sargent, K. A., 1965, Geologic map of the Skull Mountain quadrangle, Nye County, Nevada: U.S. Geol. Survey Geol. Quad. Map GQ-387.
- Fernald, A. T., Corchary, G. S., and Williams, W. P., 1968, Surficial geologic map of Yucca Flat, Nye and Lincoln Counties, Nevada: U.S. Geol. Survey Misc. Geol. Inv. Map I-550.
- Gibbons, A. B., Hinrichs, E. N., Hansen, W. R., and Lemke, R. W., 1963, Geology of the Rainier Mesa quadrangle, Nye County, Nevada: U.S. Geol. Survey Geol. Quad. Map GQ-215.
- Hinrichs, E. N., 1968, Geologic map of the Camp Desert

- Rock quadrangle, Nye County, Nevada: U.S. Geol. Survey Geol. Quad. Map GQ-726.
- Hinrichs, E. N., Krushensky, R. D., and Luft, S. J., 1967, Geologic map of Ammonia Tanks quadrangle, Nye County, Nevada: U.S. Geol. Survey Geol. Quad. Map GQ-638.
- Hinrichs, E. N., and McKay, E. J., 1965, Geologic map of the Plutonium Valley quadrangle, Nye and Lincoln Counties, Nevada: U.S. Geol. Survey Geol. Quad. Map GQ-384.
- Houser, F. N., and Poole, F. G., 1960, Preliminary geologic map of the Climax stock and vicinity: U.S. Geol. Survey Misc. Geol. Inv. Map I-328.
- Kistler, R. W., 1968, Potassium-argon ages of volcanic rocks in Nye and Esmeralda Counties, Nevada: Geol. Soc. America Mem. 110, p. 251-261.
- Lipman, P. W., and McKay, E. J., 1965, Geologic map of the Topopah Spring SW quadrangle, Nye County, Nevada: U.S. Geol. Survey Geol. Quad. Map GQ-439.
- Lipman, P. W., Quinlivan, W. D., Carr, W. J., and Anderson, R. E., 1966, Geologic map of the Thirsty Canyon SE quadrangle, Nye County, Nevada: U.S. Geol. Survey Geol. Quad. Map GQ-489.
- Luft, S. J., 1964, Mafic lavas of Dome Mountain, Timber Mountain caldera, southern Nevada, in Geological Survey research 1964: U.S. Geol. Survey Prof. Paper 501-D, p. D14-D21.
- Marvin, R. F., Byers, F. M., Jr., Mehnert, H. H., Orkild, P. P., and Stern, T. W., 1970, Radiometric ages and stratigraphic sequence of volcanic and plutonic rocks, southern Nye and western Lincoln Counties, Nevada: Geol. Soc. America Bull., v. 81, p. 2657-2676.
- McKay, E. J., Sargent, K. A., and Burchfiel, B. C., 1970, Geologic map of the Lathrop Wells quadrangle, Nye County, Nevada: U.S. Geol. Survey Geol. Quad. Map GQ-883.
- McKay, E. J., and Williams, W. P., 1964, Geology of the Jackass Flats quadrangle, Nye County, Nevada: U.S. Geol. Survey Geol. Quad. Map GQ-368.
- Noble, D. C., and Christiansen, R. L., 1968, Geologic map of the Black Mountain SW quadrangle, Nye County, Nevada: U.S. Geol. Survey Misc. Geol. Inv. Map I-562.
- Noble, D. C., Krushensky, R. D., McKay, E. J., and Ege, J. R., 1967, Geologic map of the Dead Horse Flat quadrangle, Nye County, Nevada: U.S. Geol. Survey Geol. Quad. Map GQ-614.
- O'Connor, J. T., Anderson, R. E., and Lipman, P. W., 1966, Geologic map of the Thirsty Canyon quadrangle, Nye County, Nevada: U.S. Geol. Survey Geol. Quad. Map GQ-524.
- Orkild, P. P., 1963, Geologic map of the Tippipah Spring quadrangle, Nye County, Nevada: U.S. Geol. Survey Geol. Quad. Map GQ-213.
- , 1968, Geologic map of the Mine Mountain quadrangle, Nye County, Nevada: U.S. Geol. Survey Geol. Quad. Map GQ-746.
- Orkild, P. P., and O'Connor, J. T., 1970, Geology of the Topopah Spring quadrangle, Nye County, Nevada: U.S. Geol. Survey Geol. Quad. Map GQ-849.
- Orkild, P. P., Sargent, K. A., and Snyder, R. P., 1969, Geologic map of Pahute Mesa, Nevada Test Site, Nye County, Nevada: U.S. Geol. Survey Misc. Geol. Inv. Map I-567.
- Poole, F. G., 1965, Geologic map of the Frenchman Flat quadrangle, Nye, Lincoln, and Clark Counties, Nevada: U.S. Geol. Survey Geol. Quad. Map GQ-456.
- Poole, F. G., Elston, D. P., and Carr, W. J., 1965, Geologic map of the Cane Spring quadrangle, Nye County, Nevada: U.S. Geol. Survey Geol. Quad. Map GQ-455.
- Rittmann, Alfred, 1952, Nomenclature of volcanic rocks: Bull. Volcanol., ser. 2, v. 12, p. 75-102.
- Rogers, C. L., Anderson, R. E., Ekren, E. B., and O'Connor, J. T., 1967, Geologic map of the Quartzite Mountain quadrangle, Nye County, Nevada: U.S. Geol. Survey Geol. Quad. Map GQ-672.
- Rogers, C. L., Ekren, E. B., Noble, D. C., and Weir, J. E., 1968, Geologic map of the northern half of the Black Mountain quadrangle, Nye County, Nevada: U.S. Geol. Survey Misc. Geol. Inv. Map I-545.
- Rogers, C. L., and Noble, D. C., 1969, Geologic map of the Oak Spring Butte quadrangle, Nye County, Nevada: U.S. Geol. Survey Geol. Quad. Map GQ-822.
- Ross, C. S., and Smith, R. L., 1961, Ash-flow tuffs—Their origin, geologic relations and identification: U.S. Geol. Survey Prof. Paper 366, 81 p.
- Sargent, K. A., Luft, S. J., Gibbons, A. B., and Hoover, D. L., 1966, Geologic map of the Quartet Dome quadrangle, Nye County, Nevada: U.S. Geol. Survey Geol. Quad. Map GQ-496.
- Sargent, K. A., McKay, E. J., and Burchfiel, B. C., 1970, Geologic map of the Striped Hills quadrangle, Nye County, Nevada: U.S. Geol. Survey Geol. Quad. Map GQ-882.
- Sargent, K. A., and Orkild, P. P., 1973, Geologic map of the Wheelbarrow Peak-Rainier Mesa area, Nye County, Nevada: U.S. Geol. Survey Misc. Geol. Inv. Map I-754.
- Sargent, K. A., and Stewart, J. H., 1971, Geologic map of the Specter Range NW quadrangle, Nye County, Nevada: U.S. Geol. Survey Geol. Quad. Map GQ-884.
- Smith, R. L., 1960, Ash flows: Geol. Soc. America Bull., v. 71, p. 795-842.
- Williams, Howel, 1941, Calderas and their origin: California Univ. Dept. Geol. Sci. Bull., v. 25, p. 239-346.